NATIONAL ADVISORY COMMITTEE FOR AERONAUTICS
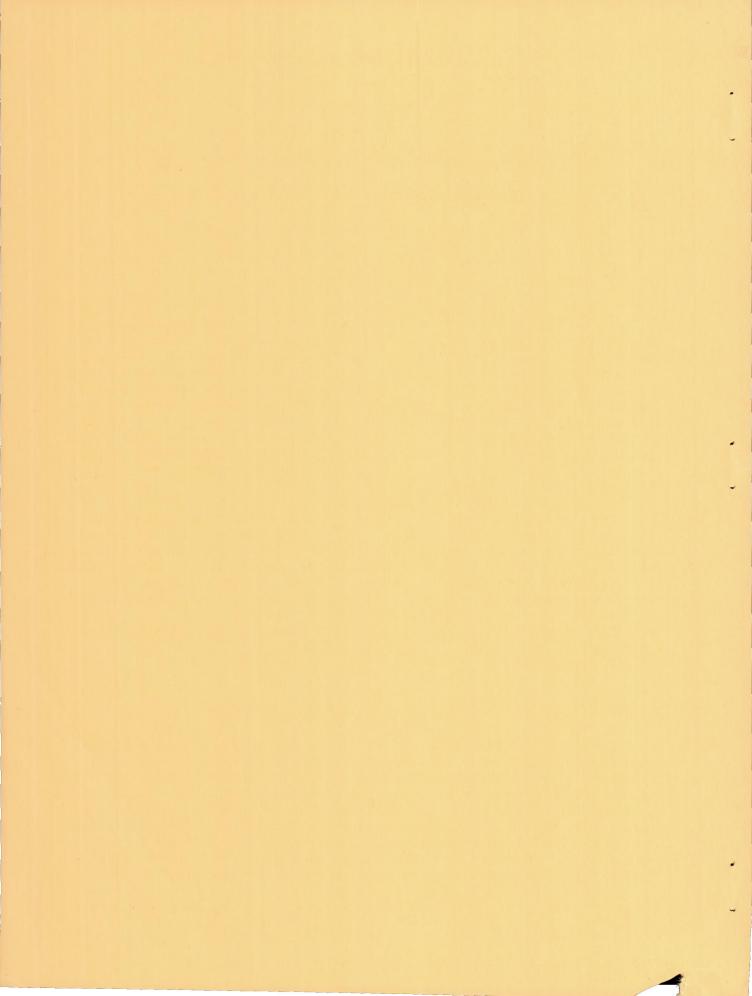
TECHNICAL NOTE 4345

SIMILAR SOLUTIONS FOR THE COMPRESSIBLE BOUNDARY LAYER

ON A YAWED CYLINDER WITH TRANSPIRATION COOLING

By Ivan E. Beckwith

Langley Aeronautical Laboratory
Langley Field, Va.

NACA

NATIONAL ADVISORY COMMITTEE FOR AERONAUTICS

TECHNICAL NOTE 4345

SIMILAR SOLUTIONS FOR THE COMPRESSIBLE BOUNDARY LAYER

ON A YAWED CYLINDER WITH TRANSPIRATION COOLING

By Ivan E. Beckwith

SUMMARY

Heat-transfer and skin-friction parameters obtained from exact
numerical solutions to the laminar compressible-boundary-layer equations
for the infinite cylinder in yaw are presented. The chordwise flow in
the transformed plane is of the Falkner-Skan type. Solutions are given
for chordwise stagnation flow with both a porous and a nonporous wall.
The effect of a linear viscosity-temperature relation is compared with
the effect of the Sutherland viscosity-temperature relation at the stag-
nation line of the cylinder for a Prandtl number of 0.7. The effects of
pressure gradient, Mach number, yaw angle, and wall temperature are inves-
tigated for a linear viscosity-temperature relation and a Prandtl number
of 1.0 with a nonporous wall.

The results indicate that compressibility effects become important
at large Mach numbers and yaw angles, with larger percentage effects on
the skin friction than on the heat transfer. The use of the two different
viscosity relations gives about the same results except when large changes
in temperature occur across the boundary layer, as for a highly cooled
wall. The present solutions predict that a larger amount of coolant would
be required at a given large Mach number and yaw angle than would be pre-
dicted from solutions of the corresponding incompressible-boundary-layer
equations.

INTRODUCTION

The so-called similar solutions of the laminar-boundary-layer equa-
tions are obtained by imposing certain restrictions on the external flow
and the wall temperature and assuming that the dimensionless profiles of
velocity and temperature are functions of a single variable. The governing
partial differential equations then reduce to ordinary equations, and the
qualitative effect of various parameters on the boundary-layer character-
istics can be investigated with much less computing labor than for the more
general case. The similar solutions are also useful as a check on the
accuracy of approximate integral methods and as the basic information for

constructing approximate methods of the piecewise type, such as those of references 1 to 3. Furthermore, the similar solutions are exact for a few physically real flows, such as those which occur on flat plates, the stagnation region of cylinders and bodies of revolution, and wedges in flows with constant fluid properties.

Similar solutions for constant-property flows are given, for example, in references 4 and 5, where the effects of pressure gradient on the velocity profiles and skin friction are considered. Solutions for the corresponding temperature profiles and heat transfer are given by Squire and Sibulkin for stagnation-type flows (refs. 6 and 7) and for various pressure and wall-temperature gradients by Schuh and Levy (refs. 8 and 9). The effects of transpiration cooling in constant-property flows are given in reference 10.

In references 11 and 12 the fluid properties were assumed to vary as powers of the temperature; solutions with transpiration cooling were included, but the results apply only to low-speed flows. In references 13 and 14 the product $\rho\mu$ of density and viscosity was assumed to be constant in accordance with the perfect-gas law and a linear variation of viscosity with temperature. These solutions are not restricted to low-speed flows when the Prandtl number is 1.0. Several solutions with transpiration cooling were included in reference 13. The effects of transpiration cooling on the heat transfer at the stagnation point of cylinders and bodies of revolution is presented in reference 15 for a constant value of $\rho\mu$ and a Prandtl number of 0.7.

The boundary layer on infinite cylinders in yaw can also be treated by the methods of similarity; and, in fact, for constant-property fluids the chordwise flow is independent of the spanwise flow, which can then be calculated by using the solutions already available for two-dimensional cylinders. (See, for example, ref. 16.) When the fluid properties are allowed to vary, the chordwise flow is no longer independent of the span-wise flow and the equations for the two components must be solved simultaneously. This problem has been considered by Crabtree (ref. 17) and Moore (ref. 18) for a constant value of $\rho\mu$, zero heat transfer, and a Prandtl number of 1.0; solutions are given for small values of the yaw-angle parameter λ in reference 19. Solutions for finite heat transfer and small values of λ are given in reference 20. In reference 21 solutions are given for the flow at or near the stagnation line with finite heat transfer and large values of λ for Prandtl numbers of 1.0 and 0.7. Solutions for the case of large suction but small values of λ and a Prandtl number of 1.0 are given in reference 22.

Fay and Riddell (ref. 23) present solutions for the flow of a real gas, including the effects of dissociation, at a three-dimensional stagnation point. They conclude, for example, that, when the Lewis number is near 1, a heat-transfer parameter in terms of a local Nusselt number and

Reynolds number depends mainly on the total variation of $\rho\mu$ across the boundary layer. For high cooling rates the effect of fluid properties becomes more important. Thus, for a ratio of wall enthalpy to local stream enthalpy of 0.05, the heat-transfer parameter is about 65 percent of the value predicted by reference 15 for a constant value of $\rho\mu$.

In the present paper the effects of wall temperature, Mach number, fluid properties, and transpiration cooling on the heat transfer and skin friction of yawed infinite cylinders are considered. The external flow in the transformed plane is required to vary as a power of the chordwise distance from the leading edge or stagnation line; the injected gas is the same as the boundary-layer gas, that is, the gas is homogeneous throughout; and the wall temperature is constant. The density variation is given by the perfect-gas law, and the specific heat and Prandtl number are assumed to be constant. Solutions are presented for Prandtl numbers of 0.7 and 1.0, for ratios of wall temperature to stagnation temperature from 0 to 1.0, and for values of the yaw-angle parameter up to 11.0. For a Prandtl number of 1.0 and a linear-viscosity-temperature relation, the pressure gradient is varied from the infinitely favorable to the value for chordwise separation. For the flow at the stagnation line of the cylinder, solutions are calculated by using both the Sutherland and the linear viscosity-temperature relations. Numerical examples are given to illustrate the effect of yaw angle and viscosity relation on the quantity of coolant required to maintain a given wall temperature.

SYMBOLS

A,B,K   arbitrary constants

a   speed of sound

$\bar{a},\bar{b}$ constants in interpolation formula for t_{aw} (eq. (48))

C   constant in Falkner-Skan velocity distribution (eq. (1a))

c_p specific heat at constant pressure

f   chordwise velocity function; related to stream function by equation (A11)

g   spanwise velocity profile function, v/v_e

H   stagnation enthalpy, $c_p T + \dfrac{u^2 + v^2}{2}$

$$h = \frac{q_w}{T_{aw} - T_w}$$

$\bar{h}$ heat-transfer-coefficient parameter (eq. (40))

i static enthalpy

k thermal conductivity

l reference length

M Mach number based on resultant or total component of flow

m exponent in Falkner-Skan velocity distribution (eq. (1a))

N_{Nu} local Nusselt number, hx/k_w

N_{Pr} Prandtl number, $c_p\mu/k$

p pressure

q heat-transfer rate per unit area

R constant in perfect-gas law (eq. (A3))

R_e local Reynolds number, $\dfrac{\rho_w u_e x}{\mu_w}$

r recovery factor (eq. (43))

S Sutherland constant (eq. (A2))

$$s = \frac{S}{T_t}$$

T temperature, $^{\circ}R$

$$t = \frac{T}{T_t}$$

U,W chordwise and normal velocities, respectively, in transformed plane (eq. (B1))

u,v,w chordwise, spanwise, and normal velocities, respectively, in physical plane

u_r resultant velocity component, $\left(u^2 + v^2\right)^{1/2}$

X,Z transformed coordinates (eq. (A7))

x,y,z chordwise, spanwise, and normal boundary-layer coordinates, respectively, in physical plane

$\bar{\alpha},\bar{\beta},\bar{\gamma}$ constants in interpolation formula for $\bar{h}$ (eq. (47))

α acute angle in chordwise plane between line tangent to surface and free-stream direction

$\beta = \dfrac{2m}{m + 1}$

γ ratio of specific heats

$\zeta = \dfrac{t_s}{t_s - \dfrac{\gamma - 1}{2}\left(\dfrac{u_e}{a_t}\right)^2} \dfrac{1}{\beta \nu_w} \dfrac{du_e}{dx}$

η similarity variable (eq. (A10))

θ enthalpy profile function, $\dfrac{H - H_w}{H_e - H_w}$

$\theta^*,\delta^*,G,E,\Theta,\Theta^*$ integral-thickness parameters in transformed plane (eqs. (B13))

Λ angle of yaw (complement of acute angle between free-stream flow direction and cylinder axis)

λ yaw-angle parameter; ratio of total stagnation temperature to stagnation temperature of flow component normal to cylinder

μ viscosity coefficient

ν coefficient of kinematic viscosity, μ/ρ

ρ mass density

τ shear stress

$\phi = \dfrac{\rho\mu}{\rho_w \mu_w}$

ψ stream function

ω coolant mass flow per unit area, $\rho_w w_w$

$\bar{\omega}$ dimensionless coolant-flow ratio, $\dfrac{\rho_w w_w}{\rho_\infty u_{r,\infty}}$

Subscripts:

e   local flow outside boundary layer (unless otherwise noted)

t   total stagnation conditions in free stream

w   wall

s   external flow at stagnation line of cylinder

∞ ahead of bow shock

aw   adiabatic wall

c   coolant

tr   transformed similarity plane

p   physical plane

st   static

A prime denotes differentiation with respect to η.

EQUATIONS AND CONDITIONS FOR SIMILAR SOLUTIONS

The general boundary-layer equations for the infinite cylinder in yaw reduce to ordinary differential equations when the dimensionless velocity and enthalpy profiles are assumed to be functions of a similarity variable and when certain restrictions are imposed on the external flow conditions and the gas properties. (See appendix A.) The external flow in the transformed coordinate system is restricted to the Falkner-Skan type:

$$U_e = CX^m \tag{1a}$$

where C and m are constants. In terms of the physical flow this relation may be expressed as

$$u_e = C \frac{a_e}{a_t} \left(\int_0^x \frac{\mu_w}{\mu_t} \frac{\rho_w}{\rho_t} \frac{a_e}{a_t} \, dx \right)^m \tag{1b}$$

from the definitions of U_e and X. The local speed of sound a_e may be written as

$$a_e = a_t \sqrt{t_s - \frac{\gamma - 1}{2} \left(\frac{u_e}{a_t} \right)^2} \tag{2}$$

from the definition of t_s and the use of the adiabatic-energy equation in the external flow. The parameter t_s depends on the stream Mach number and yaw angle as given by the expression

$$t_s = \frac{1 + \frac{\gamma - 1}{2} M_\infty^2 \cos^2 \Lambda}{1 + \frac{\gamma - 1}{2} M_\infty^2} \tag{3}$$

The so-called similar solutions can be classified into two general categories depending upon the additional restrictions used. In the first of these categories (subsequently referred to as class I flows), the chordwise velocity u_e is zero or negligible in comparison with the speed of sound. Such flows exist at or in the vicinity of a stagnation point or line and on a cylinder at very large yaw angles. The second category (class II flows) is obtained when the value of u_e is arbitrary.

Further restrictions and assumptions which, in the present investigation, apply to both categories are

(1) Prandtl boundary-layer equations for the steady flow of a homogeneous gas

(2) Perfect-gas law

(3) Constant specific heat and Prandtl number

(4) Constant wall temperature

Class I Flows

The final ordinary differential equations for class I flows subject to the restrictions and assumptions listed previously are as follows (see appendix A for derivation):

$$(\phi f'')' + f''f = \beta \left\{ (f')^2 - \frac{1}{t_s}\left[\left(1 - t_w\right)\theta - \left(1 - t_s\right)g^2 + t_w \right] \right\} \qquad (4)$$

$$(\phi g')' + fg' = 0 \qquad (5)$$

$$(\phi\theta')' + N_{Pr}f\theta' = \left(1 - N_{Pr}\right)\frac{1 - t_s}{1 - t_w}\left[\phi(g^2)'\right]' \qquad (6)$$

where the prime denotes differentiation with respect to the similarity variable η. The boundary conditions on equations (4) to (6) are, at $\eta = 0$,

$$f = -w_w\left(\frac{\nu_w}{\beta}\frac{du_e}{dx}\right)^{-1/2} \qquad (7)$$

where $f = 0$ for a nonporous wall and

$$f' = \theta = g = 0 \qquad (8)$$

As $\eta \to \infty$,

$$f' = \theta = g = 1 \qquad (9)$$

For zero aerodynamic heat transfer the additional condition required to determine the wall temperature is that $\theta'_w = 0$.

The general expression for the viscosity function ϕ is

$$\phi = \frac{\mu}{\mu_w}t_w\left[\left(1 - t_w\right)\theta - \left(1 - t_s\right)g^2 + t_w\right]^{-1} \qquad (10)$$

which, after introduction of the Sutherland viscosity relation, becomes

$$\phi = \frac{\left(t_w + s\right)\left[1 + \left(\frac{1}{t_w} - 1\right)\theta - \frac{1}{t_w}\left(1 - t_s\right)g^2\right]^{1/2}}{t_w + s + \left(1 - t_w\right)\theta - \left(1 - t_s\right)g^2} \qquad (10a)$$

If the viscosity is assumed to vary linearly with temperature according to the relation

$$\mu = \frac{\mu_w}{T_w} T$$

equation (10) is reduced to

$$\phi = 1 \tag{10b}$$

The functions f', g, and θ are the dimensionless chordwise velocity, spanwise velocity, and enthalpy profiles, respectively. The normal velocity at the wall w_w is determined from equation (7), where f_w must be a constant.

Class II Flows

For class II flows the chordwise velocity may have any value so long as equation (1b) is satisfied and the additional restrictions of $N_{Pr} = 1.0$ and $\phi = 1.0$ are imposed. (See appendix A.) The equations with these conditions are

$$f''' + f''f = \beta \left\{ (f')^2 - \frac{1}{t_s} \left[(1 - t_w)\theta - (1 - t_s)g^2 + t_w \right] \right\} \tag{11}$$

$$g'' + fg' = 0 \tag{12}$$

$$\theta'' + f\theta' = 0 \tag{13}$$

For equations (11) to (13) the boundary conditions are, at $\eta = 0$,

$$f = -w_w \left[\frac{v_w}{\beta} \left(1 + \frac{\gamma - 1}{2} \frac{u_e^2}{a_e^2} \right) \frac{du_e}{dx} \right]^{-1/2} \tag{14}$$

$$f' = \theta = g = 0 \tag{15}$$

and, at $\eta \rightarrow \infty$,

$$f' = \theta = g = 1 \tag{16}$$

Inasmuch as the spanwise velocity profile g is exactly the same as the enthalpy profile θ, equations (11) to (13) reduce to a fifth-order system. The normal velocity at the wall w_w is

$$w_w = -f_w \left[\frac{\nu_w}{\beta} \left(1 + \frac{\gamma - 1}{2} \frac{u_e^2}{a_e^2} \right) \frac{du_e}{dx} \right]^{1/2} \tag{17}$$

from equation (14), where again f_w must be constant.

GENERAL EXPRESSIONS FOR HEAT TRANSFER AND SKIN FRICTION

Transformation Relations Between z and η

Since expressions for the heat transfer and skin friction involve derivatives normal to the wall, it is useful to consider the transformation from the physical xz-plane to the similarity plane $X\eta$. From appendix A the normal derivative is

$$\frac{\partial}{\partial z} = \frac{a_e}{a_t} \frac{\rho}{\rho_t} \sqrt{\frac{m + 1}{2} \frac{U_e}{\nu_t X}} \frac{\partial}{\partial \eta} \tag{18}$$

Differentiation of equation (1b) written in the form

$$u_e = C \left[t_s - \frac{\gamma - 1}{2} \left(\frac{u_e}{a_t} \right)^2 \right]^{1/2} X^m$$

and the use of the Stewartson transformation yield

$$\frac{U_e}{X} = \frac{t_s}{m} \left(\frac{a_t}{a_e} \right)^4 \frac{\mu_t \rho_t}{\mu_w \rho_w} \frac{du_e}{dx} \tag{19}$$

Substituting equation (19) into equation (18) and evaluating at the wall then give

$$\left(\frac{\partial}{\partial z} \right)_w = \left[\frac{t_s}{t_s - \frac{\gamma - 1}{2} \left(\frac{u_e}{a_t} \right)^2} \frac{1}{\beta \nu_w} \frac{du_e}{dx} \right]^{1/2} \left(\frac{\partial}{\partial \eta} \right)_w$$

or for brevity

$$\left(\frac{\partial}{\partial z}\right)_w = \sqrt{\zeta}\left(\frac{\partial}{\partial \eta}\right)_w \tag{20}$$

where ζ is a function of x only. Similarily, it can be shown that for a given x-station the relation between z and η is

$$z = \frac{1}{t_w\sqrt{\zeta}} \int_0^\eta t \; d\eta \tag{21}$$

where the temperature ratio t is, in general,

$$t = \left(1 - t_w\right)\theta - \left(1 - t_s\right)g^2 + t_w - \frac{\gamma - 1}{2}\left(\frac{u_e}{a_t}\right)^2 (f')^2 \tag{22}$$

Local Heat Transfer and Skin Friction

The heat-transfer rate per unit area at the wall is

$$q_w = k_w\left(\frac{\partial T}{\partial z}\right)_w$$

which, from the definitions of H and θ, may be written as

$$q_w = k_w\left(T_t - T_w\right)\left(\frac{\partial \theta}{\partial z}\right)_w$$

Then from equation (20)

$$q_w = k_w\left(T_t - T_w\right)\sqrt{\zeta}\,\theta'_w \tag{23}$$

Combining equations (23) and (14) yields the relation

$$q_w = -\frac{c_p}{N_{Pr}} \frac{\rho_w w_w}{f_w}\left(T_t - T_w\right)\theta'_w \tag{23a}$$

which shows that for a given similar flow q_w varies with x directly as the coolant mass flow since θ'_w and f_w are independent of x.

From equation (23) the expression for the local heat-transfer parameter $N_{Nu}/\sqrt{R_e}$ is

$$\frac{N_{Nu}}{\sqrt{R_e}} \equiv \frac{hx/k_w}{\sqrt{\rho_w u_e x/\mu_w}} = \left[\frac{t_s}{t_s - \frac{\gamma - 1}{2}\left(\frac{u_e}{a_t}\right)^2} \frac{x}{\beta u_e} \frac{du_e}{dx}\right]^{1/2} \frac{T_t - T_w}{T_{aw} - T_w} \theta'_w \quad (24)$$

Equation (24) may also be written in a form that does not include a velocity-gradient term by using equation (18) directly in the expression for q_w preceding equation (23). After the definitions of β and X are introduced, the result is

$$\frac{N_{Nu}}{\sqrt{R_e}} = \left(\frac{1}{2 - \beta} \frac{\frac{\mu_w \rho_w}{\mu_t \rho_t} \frac{a_e}{a_t} x}{\int_0^x \frac{\mu_w \rho_w}{\mu_t \rho_t} \frac{a_e}{a_t} dx}\right)^{1/2} \frac{T_t - T_w}{T_{aw} - T_w} \theta'_w \quad (24a)$$

When $x \to 0$, as at a stagnation line, equation (24a) reduces, in the limit, to

$$\frac{N_{Nu}}{\sqrt{R_e}} = \frac{1}{\sqrt{2 - \beta}} \frac{T_t - T_w}{T_{aw} - T_w} \theta'_w \quad (24b)$$

A heat-transfer parameter which for given stream conditions is proportional to the heat-transfer coefficient h may be written as

$$\frac{hl/k_\infty}{\sqrt{\rho_\infty u_{r,\infty} l/\mu_\infty}} = \left[\frac{\rho_w \mu_w}{\rho_\infty \mu_\infty} \frac{\cos \Lambda}{\beta} \left(\frac{l}{u_\infty} \frac{du_e}{dx}\right)\left(\frac{t_s}{t_s - \frac{\gamma - 1}{2} \frac{u_e^2}{a_t^2}}\right)\right]^{1/2} \frac{T_t - T_w}{T_{aw} - T_w} \theta'_w \quad (25)$$

from equation (24) and the assumption that $k_w/k_\infty = \mu_w/\mu_\infty$.

The expressions for local chordwise and spanwise skin friction may be written as

$$\tau_{ch} = \mu_w\left(\frac{\partial u}{\partial z}\right)_w = \mu_w u_e \sqrt{\zeta} f''_w \quad (26)$$

$$\tau_{sp} = \mu_w\left(\frac{\partial v}{\partial z}\right)_w = \mu_w v_e \sqrt{\zeta} g'_w \quad (27)$$

The total component of the local skin friction in the direction of the free stream is then

$$\tau_{total} = \mu_w \sqrt{\zeta} \left(f_w'' \cos \alpha \cos \Lambda + g_w' \sin \Lambda \right) \tag{28}$$

where α is the angle in the chordwise plane between a line tangent to the surface and the free-stream direction.

Simplified Heat Balance

In the absence of lateral heat conduction within the porous wall and heat loss by radiation, all the heat transferred to the wall by the airstream must be absorbed by the coolant. If the coolant flow through the porous wall is assumed normal to the wall throughout and the aerodynamic heat transfer is given by equation (23), the resulting heat balance is

$$k_w \left(T_t - T_w \right) \sqrt{\zeta} \theta_w' = \rho_w w_w c_p \left(T_w - T_c \right) \tag{29}$$

where T_c is the initial temperature of the coolant before it enters the porous wall. Rearranging equation (29) and introducing f_w from equation (14) and a_e from equation (2) give a relation between the pertinent temperatures and the parameters θ_w' and f_w involved in the similar solutions. This relation is

$$\frac{T_t - T_w}{T_w - T_c} \frac{\theta_w'}{N_{Pr}} = -f_w \tag{30}$$

which, if any two of the three quantities T_w, T_c, or f_w are known, determines the remaining unknown value since θ_w' depends only on t_w and f_w for given stream conditions and yaw angle. Typical problems utilizing equation (30) would be to find the wall temperature from given coolant temperature and mass flow or to find the coolant flow required to maintain a given wall temperature. The latter problem is considered in some detail in the section entitled "Results and Discussion."

If radiation and conduction are included, a more general heat balance, such as that given in references 1 and 15, must be used.

BOUNDARY-LAYER-THICKNESS PARAMETERS

Transformed Plane

In various applications of the present results it is convenient to have available certain boundary-layer-thickness parameters which are obtained from integration of the velocity or enthalpy profiles over the boundary-layer thickness. These parameters are defined in the XZ-plane since transformation to this plane results in considerable simplification of any compressible-boundary-layer calculation. The particular parameters included in the tabulated results of the present report are those that appear in the integral boundary-layer equations which are derived in appendix B.

Transformation from the general Stewartson variable Z to the similarity variable η (see appendix A) requires that any thickness parameter in the XZ-plane can be obtained by multiplying the corresponding parameter in the similarity plane by the quantity

$$\sqrt{\frac{2}{m+1} \frac{\nu_t X}{U_e}}$$

Thus, for example, the displacement thickness δ^* in the XZ-plane is defined as

$$\delta^* = \int_0^\infty \left(1 - \frac{U}{U_e}\right) dZ$$

or, after transformation to the similarity variable,

$$\delta^* = \sqrt{\frac{2}{m+1} \frac{\nu_t X}{U_e}} \int_0^\infty (1 - f') d\eta = \sqrt{\frac{2}{m+1} \frac{\nu_t X}{U_e}} \delta^*_{tr}$$

Performing the indicated integration then yields the following expression for the displacement thickness δ^*_{tr} in the similarity plane:

$$\delta^*_{tr} \equiv \lim_{\eta_e \to \infty} \int_0^{\eta_e} (1 - f') d\eta = \lim_{\eta_e \to \infty} \left(\eta_e - f_e + f_w\right) \qquad (31)$$

Similarly, the momentum thickness is defined as

$$\theta_{tr}^* \equiv \lim_{\eta_e \to \infty} \int_0^{\eta_e} \left[f' - (f')^2 \right] d\eta = \lim_{\eta_e \to \infty} \left[f_e - f_w - \int_0^{\eta_e} (f')^2 d\eta \right]$$

which, after integration of the last term by parts and introduction of ff'' from equation (4), becomes

$$\theta_{tr}^* = \lim_{\eta_e \to \infty} \frac{1}{1 + \beta} \left[f_w'' - f_w - \beta \left(f_w + \eta - f_e \right) - \beta \left(\frac{1}{t_s} - 1 \right) \int_0^{\eta_e} \left(1 - g^2 \right) d\eta - \right.$$

$$\left. \beta \frac{1}{t_s} \left(t_w - 1 \right) \int_0^{\eta_e} \left(1 - \theta \right) d\eta \right] \tag{32}$$

A spanwise parameter G_{tr} is defined as

$$G_{tr} = \lim_{\eta_e \to \infty} \int_0^{\eta_e} \left(1 - g^2 \right) d\eta \tag{33}$$

which is the sum of the spanwise displacement and momentum thicknesses.

The thermal thickness is defined as

$$\Theta_{tr}^* = \lim_{\eta_e \to \infty} \int_0^{\eta_e} (1 - \theta) d\eta \tag{34}$$

The final form of the momentum thickness is then obtained by substituting equations (31), (33), and (34) into equation (32), which becomes

$$\theta_{tr}^* = \frac{f_w'' - f_w}{1 + \beta} - \frac{\beta}{1 + \beta} \left[\delta_{tr}^* + \left(\frac{1}{t_s} - 1 \right) G_{tr} + \frac{1}{t_s} \left(t_w - 1 \right) \Theta_{tr}^* \right] \tag{35}$$

The remaining parameters appearing in the integral equations (appendix B) may be considered as convection thicknesses when the analogy between g and θ $\left(\text{for } N_{Pr} = 1 \right)$ is considered. The spanwise convection thickness or "mixed" momentum thickness is defined as

$$E_{tr} \equiv \lim_{\eta_e \to \infty} \int_0^{\eta_e} f'(1 - g)d\eta = \lim_{\eta_e \to \infty} \left(f_e - f_w - \int_0^{\eta_e} gf'd\eta \right)$$

Integrating the last term by parts and using equation (5) result in

$$E_{tr} = g_w' - f_w \tag{36}$$

Likewise, the enthalpy convection thickness is

$$\Theta_{tr} = \lim_{\eta_e \to \infty} \int_0^{\eta_e} f'(1 - \theta)d\eta = \frac{\theta_w'}{N_{Pr}} - f_w \tag{37}$$

from integration by parts and equation (6). Equations (35), (36), and (37) show that θ_{tr}^*, E_{tr}, and Θ_{tr} can be written in terms of the derivatives of the profiles at the wall and the other three integral thicknesses δ_{tr}^*, G_{tr}, and Θ_{tr}^*.

Physical Plane

The momentum and displacement thicknesses in the physical plane can be expressed in terms of the thickness parameters in the similarity plane. The chordwise momentum thickness in the physical plane is defined as

$$\theta_p^* = \lim_{z_e \to \infty} \int_0^{z_e} \left[\frac{u}{u_e} - \left(\frac{u}{u_e} \right)^2 \right] \frac{\rho}{\rho_e} dz$$

which, from equation (21) and the perfect-gas law, may be written

$$\theta_p^* = \frac{t_e}{t_w \sqrt{\zeta}} \lim_{\eta_e \to \infty} \int_0^{\eta_e} \left[f' - (f')^2 \right] d\eta$$

since $\frac{u}{u_e} = f'$. Then, from the definition of θ_{tr}^*,

$$\theta_p^* = \frac{t_e}{t_w \sqrt{\zeta}} \theta_{tr}^* \tag{38}$$

According to reference 24, the physical displacement thickness on a yawed infinite cylinder is not affected by the spanwise mass-flow defect. Hence, the displacement thickness is defined in the usual way as

$$\delta_p^* = \lim_{z_e \to \infty} \int_0^z \left(1 - \frac{\rho u}{\rho_e u_e}\right) dz$$

which, from equation (21), the definition of δ_{tr}^*, and the perfect-gas law, may be written, after some rearranging, as

$$\delta_p^* = \lim_{\eta_e \to \infty} \left[\frac{t_e}{t_w\sqrt{\zeta}} \int_0^{\eta_e} \left(\frac{t}{t_e} - 1\right) d\eta + \delta_{tr}^*\right]$$

Substituting equation (22) for t and using equation (32) and the definition of θ_{tr}^* then yield

$$\delta_p^* = \frac{t_s}{t_w\sqrt{\zeta}} \left[\left(\frac{\gamma - 1}{2t_s} \frac{u_e^2}{a_t^2} - \frac{1 + \beta}{\beta}\right)\theta_{tr}^* + \frac{f_w'' - f_w}{\beta}\right] \tag{39}$$

COMPUTING PROCEDURE

More than 200 solutions to equations (4) to (6) and (11) to (13) have been obtained by means of the IBM type 704 electronic data processing machine. The numerical integration procedure of reference 25 was used, and the procedure described in reference 21 for obtaining convergence to the correct boundary conditions was included in the automatic programing for the machine. A step size of 0.2 in η was used for most of the solutions; however, a step size of 0.1 was used in a few solutions which are included for comparison in the tabulated results. The accuracy of the present solutions, except for $\beta > 1.0$ and $f_w < -0.5$, is believed to be as good as or better than the accuracy of the solutions in reference 21. The boundary conditions at large values of η on f', g, and θ were satisfied to within 0.0001. The solutions were carried out to sufficiently large values of η that the absolute values of the derivatives of the functions f'', g', and θ' were ≤ 0.0005. For negative values of β the absolute values of the derivatives at large values of η were ≤ 0.00005. In all solutions it was found that these requirements could be satisfied for $\eta \leq 8$. For negative values of β there is a problem of uniqueness (see, for example, refs. 4 and 14) which is discussed in relation to the present solutions in appendix C.

RESULTS AND DISCUSSION

The values of f_w'', g_w', θ_w', $\bar{h}$, δ_{tr}^*, G_{tr}, Θ_{tr}^*, and θ_{tr}^* which constitute the principal results are presented in tables I to IV for most of the solutions in the present investigation. All heat-transfer and skin-friction coefficients or parameters as well as most of the boundary-layer-thickness parameters can be derived from these tabulated values as described elsewhere in this report. The solutions included in each table are summarized as follows:

Table	β	N_{Pr}	ϕ	s	f_w	t_w	λ
I	1.0	1.0	1.0	------	0, -0.5, -1.0	0, 0.5, 1.0	1.0, 1.6, 3.0, 6.5
		0.7				0, 0.5, 1.0, t_{aw}	
II	1.0	0.7	$\neq 1.0$	0.2	0, -0.5, -1.0	0.05, 0.5, 1.0, t_{aw}	1.0, 1.6, 3.0, 6.5, 11.0
				0.02	0, -0.5, -0.75, -1.0		
III(a)	0.5	0.7	$\neq 1.0$	0.005	0	0.015, 0.050, 0.070, 0.100, 0.150, 0.200, 0.250, 0.300	1.0
				0.02		0.06, 0.20, 0.50	
				0.0625		0.1875, 0.627	
				0.2		0.05, 0.50	
III(b)	1.0	0.7	$\neq 1.0$	0.005	0	0.015, 0.050, 0.100, 0.200, 0.300	1.0
						0.015, 0.050, 0.200, t_{aw}	3.0
						0.015, 0.50, 0.200, t_{aw}	11.0
				0.0625		0.1875, 0.625	1.0
IV(a)	0.2, 0.5, 1.5, 2.0	1.0	1.0	------	0	0, 0.5, 1.0	1.0, 1.6, 3.0, 6.5
IV(b)	<0	1.0	1.0	------	0	0, 0.5, 1.0	1.0, 1.6, 3.0, 6.5

Velocity and Temperature Profiles at the Stagnation Line

Typical profiles of the chordwise and spanwise velocity ratios and the stagnation-enthalpy difference ratios are shown in figure 1. These results are for stagnation-line flow ($\beta = 1.0$), $\phi = 1.0$, $N_{Pr} = 0.7$, and $t_w = 0.5$. Note that a given change in the transpiration-cooling

parameter f_w has a larger effect on the g and θ profiles (figs. 1(b) and 1(c)) than on the f' profiles (fig. 1(a)) and that these effects tend to diminish as λ is increased. Inspection of tables I and II shows that the same trends are present in the derivatives of the profiles at the wall. Comparison of figures 1(b) and 1(c) shows that the g and θ profiles are nearly identical for $N_{Pr} = 0.7$. According to previous discussion these profiles are identical when $N_{Pr} = 1.0$.

The temperature profile at the stagnation line ($x = 0$) depends only on the spanwise profile g and the enthalpy profile θ as given by equation (22). The resulting variations in the ratio of local static temperature to total stagnation temperature are shown in figure 2 for $\lambda = 1.6$ and 6.5 and for $t_w = 0$, 0.5, and t_{aw}, and $f_w = 0$, -0.5, and -1.0. This figure illustrates the large changes in temperature distribution that occur as the yaw angle is increased. The reduction in heat-transfer rate and recovery temperature with increasing coolant flow are also evident. In regard to the possibility of dissociation or other real-gas effects, it is of interest to note that for large cooling rates (small values of t_w) the maximum temperatures in the boundary layer are much lower at large values of the yaw parameter than at small values of the parameter.

Heat-Transfer Coefficients and Recovery Factors

in the Stagnation Region

Effect of yaw parameter and transpiration cooling.- Equation (25) shows that for given stream conditions, wall temperature, and yaw angle the heat-transfer coefficient depends only on the parameter $\bar{h}$, which is defined as

$$\bar{h} = \frac{T_t - T_w}{T_{aw} - T_w} \, \theta'_w \tag{40}$$

In figure 3(a), $\bar{h}$ is plotted against λ for Prandtl numbers of 1.0 and 0.7 and for $f_w = 0$, -0.5, and -1.0. The figure shows that the parameter $\bar{h}$ (and hence also the heat-transfer coefficient) is reduced considerably by increasing the magnitude of the transpiration-cooling parameter f_w, with the largest reductions being obtained for small values of λ and for $N_{Pr} = 1.0$. A change in the value of the transpiration-cooling parameter, however, would generally imply a change in the coolant mass flow and wall temperature. Equation (23a) can be written in coefficient form as

$$h = -\frac{c_\rho}{N_{Pr}} \frac{\omega}{f_w} \bar{h} \tag{41}$$

where $\omega = \rho_w w_w$. Thus, for a finite normal velocity at the wall, the heat-transfer coefficient is determined solely by the coolant mass flow and the parameters f_w and $\bar{h}$. The parameter f_w is related to the coolant mass flow by means of equation (7), which may be written as

$$f_w = \frac{-\omega}{\sqrt{\frac{\mu_w}{T_w} \frac{p_e}{R} \frac{du_e}{dx}}} \tag{42}$$

Then since the quantity $\sqrt{\mu_w/T_w}$ is nearly constant for relatively large changes in wall temperature $\left(\text{for example, a change in } T_w \text{ of } 400^\circ \text{ R}\right.$ causes only a 7-percent change in $\left.\sqrt{\mu_w/T_w}\right)$, equation (42) indicates that an increase in coolant mass flow ω would cause a corresponding increase in the magnitude of f_w, and hence, from figure 3(a), a reduction in $\bar{h}$. It then follows from equation (41), as would be expected, that increasing ω decreases the heat-transfer coefficient h. This effect is shown directly in figure 3(b) where the ratio of $\bar{h}$ with transpiration cooling to $\bar{h}$ for a nonporous wall is plotted against λ. The ratio of the heat-transfer coefficients is proportional to the ratio of the values of $\bar{h}$ for a constant value of $\rho_w \mu_w$. Figure 3(b) is not to be interpreted as indicating an increase in heat-transfer coefficient with yaw angle at a constant value of ω, since an increase in yaw angle causes a large decrease in the local density ρ_w and velocity gradient du_e/dx. Consequently, for given stream conditions and a constant value of ω, an increase in yaw angle decreases the heat-transfer coefficient.

The effect of Prandtl number on the heat-transfer coefficient is shown in figure 3(c) where the ratio of $\bar{h}$ for $N_{Pr} = 0.7$ to $\bar{h}$ for $N_{Pr} = 1.0$ is plotted against λ. This figure shows that the approximate expression

$$\frac{\bar{h}_{0.7}}{\bar{h}_{1.0}} \approx \left(N_{Pr}\right)^{0.4}$$

suggested in reference 21 is adequate for a nonporous wall but is in considerable error for transpiration cooling.

The recovery factor or recovery temperature must be known before heat-transfer rates can be calculated from heat-transfer coefficients. The recovery factor r defined at the stagnation line as

$$r = \frac{T_{aw} - T_s}{T_t - T_s} \tag{43}$$

is plotted against the coolant parameter f_w in figure 4. The variation of the recovery factor for a flat plate from reference 1 is also shown for comparison. Increasing the coolant flow decreases the recovery factor on both the yawed cylinder and the flat plate. On the yawed cylinder, larger decreases in the recovery factor are obtained for small values of λ than for large values of λ. The recovery factor on the flat plate is, of course, independent of the yaw parameter.

Effect of viscosity assumption.- The ratio of the heat-transfer parameter $\bar{h}$ from the solutions calculated by using the Sutherland viscosity relation to the corresponding value of $\bar{h}$ for $\phi = 1.0$ is plotted against λ in figure 5 for $N_{Pr} = 0.7$ and $\beta = 1.0$. Three parameters must be considered: the transpiration-cooling parameter f_w, the ratio of wall temperature to stagnation temperature t_w, and the ratio of the Sutherland constant to stagnation temperature $s = S/T_t$. If the value of S is taken as 200° R, then $s = 0.2$ corresponds to ordinary wind-tunnel conditions with $T_t = 1,000^\circ$ R or to flight conditions with $T_\infty \approx 400^\circ$ R and $M_\infty \approx 3$, while $s = 0.02$ corresponds to $T_t = 10,000^\circ$ R or to flight conditions at $M_\infty \approx 11.0$.

All results from the solutions for $t_w = 0.5$ fall within the shaded band in the center of figure 5. For $\lambda > 3$ and $t_w \gtrsim 0.5$, the linear viscosity relation gives practically the same results as the more accurate Sutherland relation. For $\lambda < 3$ and $t_w \gtrsim 0.5$ the linear viscosity relation results in heat-transfer coefficients that are as much as 15 percent larger than those obtained with the Sutherland relation. From a comparison of the values of $\bar{h}$ listed in tables I and II, the largest deviations are seen to occur when $s = 0.02$, which for $t_w = 0.5$ is beyond the range of practical wall temperatures. For $s = 0.2$ and $t_w = 0.5$ the maximum differences resulting from the use of the two viscosity relations is about 10 percent.

For $t_w = 0.05$, a value corresponding to large aerodynamic heat-transfer rates, the viscosity relation has a large effect for both values of s. When $s = 0.2$ with $t_w = 0.05$, the use of the linear viscosity relation results in heat-transfer coefficients that are from 10 to 50 percent smaller, with the differences increasing as the transpiration-cooling rates are increased. For $s = 0.02$ and $t_w = 0.05$ the linear relation has the opposite effect in that the heat-transfer coefficients are from

20 to 80 percent larger, with the largest deviations occurring again at the largest values of f_w. At some intermediate value of s the viscosity assumption might be expected to have little effect even for the large heating rates. For all conditions except s = 0.2, t_w = 0.05, and f_w = 0 and -0.5 the effects of the viscosity assumption tend to become smaller as the yaw-angle parameter λ is increased.

The effect of viscosity assumption on the variation of heat-transfer coefficient with yaw angle or yaw-angle parameter may be obtained from figure 5 by noting that

$$\frac{h/h_{\Lambda=0}}{\left(h/h_{\Lambda=0}\right)_{\phi=1}} = \frac{h/h_{\phi=1}}{\left(h/h_{\phi=1}\right)_{\Lambda=0}} = \frac{\bar{h}/\bar{h}_{\phi=1}}{\left(\bar{h}/\bar{h}_{\phi=1}\right)_{\lambda=0}}$$

since from equation (25), h is proportional to $\bar{h}$, for given stream conditions, wall temperature, and yaw angle. This relation and figure 5 then indicate that (except for s = 0.2 and f_w = -1.0) when the Sutherland viscosity relation is used the predicted decrease in heat-transfer coefficient with yaw angle is somewhat smaller than when the linear viscosity relation is used.

The ratio of recovery factor r from the solutions computed by using Sutherland's relation to r for ϕ = 1.0 is plotted against λ in figure 6. This ratio is found to be essentially independent of the transpiration cooling inasmuch as all results are within the narrow bands shown in the figure. The viscosity relation has at most a 2-percent effect, which depends only on the temperature level (that is, on T_t) and is a maximum for s = 0.02 and for large values of λ.

Real-gas effects.- The assumptions of constant specific heat and density variation according to the perfect-gas law would be expected to limit the application of the present results to relatively low temperature levels where real-gas effects and, in particular, dissociation effects are not important. An indication of the limits of applicability of the present solutions may be obtained by comparison with the real-gas solutions of Fay and Riddell (ref. 23).

Since the solutions presented in reference 23 are for the stagnation point of a body of revolution, any results from the present calculations must first be transformed to the corresponding axisymmetric configuration before a valid comparison can be made.

At the stagnation point on a body of revolution, $T_{aw} = T_t$, and from the Mangler transformation the heat-transfer parameter $N_{Nu}/\sqrt{R_e}$ is

$\sqrt{3}$ times the corresponding parameter in two-dimensional flow with the velocity-gradient parameter $\beta = 0.5$. The heat-transfer parameter at the stagnation point on a body of revolution is then obtained from equation (24b) as

$$\left(\frac{N_{Nu}}{\sqrt{R_e}}\right)_{3\text{-dimensional}} = \sqrt{2}\left(\theta_w'\right)_{2\text{-dimensional}}$$

where θ_w' is taken from the solutions for the unyawed cylinder ($\lambda = 1$) with $\beta = 0.5$. The principal results of these solutions are given in table III(a), and the resulting values of the heat-transfer parameter for the stagnation point on a body of revolution are plotted in figure 7 against the ratio $\frac{\rho_s \mu_s}{\rho_w \mu_w}$. Also shown in figure 7 for comparison is the correlation given by Fay and Riddell (ref. 23) for their real-gas solutions of the equilibrium boundary layer with a Lewis number of 1. In reference 23, the Sutherland viscosity relation was used and the Prandtl number was assumed to be constant at 0.71. Since the effects of diffusion disappear from the differential equations for a Lewis number of 1.0 (see ref. 23), the only differences between the present solutions and those of reference 23 would be caused by the different assumptions for the variation of density and specific heat. The close agreement between the results of the present solutions and those of reference 23, as shown in figure 7, therefore indicates that the heat transfer at a stagnation point is not sensitive to the effects of dissociation on density and specific heat within the boundary layer. For equilibrium dissociation and a Lewis number of 1 the heat-transfer rate at a three-dimensional stagnation point can then be calculated from the equation (ref. 23)

$$q_w = \sqrt{\rho_w \mu_w \left(\frac{du_e}{dx}\right)_s} \; \frac{H_e - H_w}{N_{Pr}} \left(\frac{N_{Nu}}{\sqrt{R_e}}\right) \tag{44}$$

where all quantities would be evaluated for the real-gas conditions except $N_{Nu}/\sqrt{R_e}$, which may be taken from the appropriate solution of the boundary-layer equations for a perfect gas with a constant value of c_p and Sutherland viscosity law. The appropriate perfect-gas solution, according to the correlation of figure 7, would be the one for which the total variation of $\rho\mu$ across the boundary layer is the same as in the required real-gas conditions.

Whether this procedure can be extended to the stagnation line of a yawed cylinder is not known since the corresponding real-gas solutions

for this case are not yet available. Such an extension would appear
reasonable, however, if the perfect-gas solutions for the yawed cylinder
could be correlated in a form similar to the results for a three-
dimensional stagnation point. In order to investigate this possibility,
several additional solutions for the yawed cylinder ($\beta = 1$) were obtained
for the range of conditions used in the solutions for $\beta = 0.5$. These
results are presented in table III(b), and the heat-transfer parameter is
plotted in figure 7. For small values of s the heat-transfer parameter
for $\beta = 1$ and $\lambda = 1$ to 11 is correlated within about 4 percent by the
expression

$$\frac{N_{Nu}}{\sqrt{R_e}} = 0.5\left(\frac{\rho_s\mu_s}{\rho_w\mu_w}\right)^{0.44} \tag{45}$$

The values that are not correlated by equation (45), that is, the values
for $\lambda = 6.5$ and 11 with $s = 0.2$, are not representative of flight con-
ditions since such values occur at large Mach numbers and large yaw angles
but with $T_t \approx 1,000^\circ$ R. By analogy with the results for a three-
dimensional stagnation point, it may be assumed that the heat transfer at
the stagnation line of a yawed cylinder in a real-gas flow (with equi-
librium dissociation and a Lewis number of 1) can be calculated from
equations (44) and (45) with H_e replaced by the adiabatic wall
enthalpy H_{aw}. From equation (43), the value of H_{aw} would be

$$H_{aw} = r\left(H_e - i_s\right) + i_s$$

where, from the adiabatic-energy equation, i_s is defined as

$$i_s = H_e - \frac{1}{2}v_e^2$$

and from figures 4 and 6 the recovery factor is approximately

$$r \approx \sqrt{N_{Pr}}$$

The effect of the viscosity relation at a three-dimensional stag-
nation point can be obtained from figure 7 by comparison of the results
of reference 15 for $\frac{\rho_s\mu_s}{\rho_w\mu_w} = 1$ with the present solutions. The use of
the Sutherland viscosity relation for the range of t_w and s in the
present solutions predicts smaller values of the heat-transfer parameter
than those given by reference 15 for a linear viscosity relation. The

maximum effect is found again for small values of t_w and s; for example, with $t_w = 0.015$ and $s = 0.005$ the heat-transfer parameter is about 50 percent of the value given by reference 15.

Variation of Coolant Flow and Wall Temperature With Yaw

Angle at the Stagnation Line of a Cylinder

Interpolation formulas for $\bar{h}$.- The problem of calculating the wall temperature from given stream conditions, coolant temperature, and coolant mass flow may be solved by means of equations (30) and (42) and graphical interpolation for $\bar{h}$ and t_{aw}. The general procedure would be to assume a wall temperature and calculate a first approximation for f_w from equation (42). This value of f_w, together with the assumed wall temperature and stream conditions, is used to determine $\bar{h}$ and t_{aw} from interpolation in figures 3(a) and 4. The corresponding value of θ_w' is then used in equation (30), which is solved for T_w. Only one or two iterations would normally be required because the quantity μ_w/T_w is such a weak function of T_w.

A problem that is perhaps of more interest is to determine the quantity of coolant required to maintain a given wall temperature. Since θ_w' is a function of f_w, equation (30) has to be solved by a trial-and-error process for f_w after which the corresponding coolant mass flow is determined from equation (42). This trial-and-error process, however, would be tedious and inaccurate since interpolation for θ_w' as a function of t_w, λ, and f_w would generally be required. The limited number of solutions available, as well as the behavior of θ_w' for $T_w \rightarrow T_{aw}$, makes such an interpolation impractical. On the other hand, the function $\bar{h}$ is in the form of a coefficient and hence remains finite for all values of t_w. Thus, in order to facilitate interpolation, equation (30) is written in terms of $\bar{h}$ as

$$f_w = -\frac{T_{aw} - T_w}{T_w - T_c} \frac{\bar{h}}{N_{Pr}} \tag{46}$$

and $\bar{h}$ is assumed to have the form

$$\bar{h} = \left(\bar{\alpha}_0 t_w^2 + \bar{\beta}_0 t_w + \bar{\gamma}_0\right) f_w^2 + \left(\bar{\alpha}_1 t_w^2 + \bar{\beta}_1 t_w + \bar{\gamma}_1\right) f_w + \left(\bar{\alpha}_2 t_w^2 + \bar{\beta}_2 t_w + \bar{\gamma}_2\right)$$

$$\tag{47}$$

where $\bar{\alpha}$, $\bar{\beta}$, and $\bar{\gamma}$ are constants for any given set of λ, N_{Pr}, and s or ϕ. In general, nine exact solutions at a fixed value of λ would be required to evaluate the nine constants in equation (47). For $N_{Pr} = 1.0$, the required nine solutions are available, but for $N_{Pr} \neq 1.0$ (see tables I to III), only six solutions are available for evaluating the constants since the limiting value of $\bar{h}$ for $T_w = T_{aw}$ apparently cannot be calculated from the zero-heat-transfer solutions. However, for $N_{Pr} \neq 1.0$, the same form of equation (47) was retained by assuming that at $t_w = t_{aw}$

$$\left(\frac{\partial \bar{h}}{\partial t_w}\right)_{N_{Pr} \neq 1.0} = \left(\frac{\partial \bar{h}}{\partial t_w}\right)_{N_{Pr} = 1.0}$$

The resulting values for the constants in equation (47) for both $N_{Pr} \neq 1.0$ and $N_{Pr} = 1.0$ are given in table V. For $N_{Pr} \neq 1.0$ the recovery temperature t_{aw} is assumed to be linear in f_w (for $N_{Pr} = 1.0$, $t_{aw} = 1.0$) since from figures 4 and 6, r is linear in f_w to within about 0.25 percent. Hence, for the application of equation (46), t_{aw} is given by the equation

$$t_{aw} = \bar{a} + \bar{b}f_w \tag{48}$$

The constants $\bar{a}$ and $\bar{b}$ are also listed in table V. Combining equations (46), (47), and (48) gives a quadratic equation in f_w for $N_{Pr} = 1.0$, and for $N_{Pr} \neq 1.0$ there is obtained a cubic equation which can be easily solved for f_w by standard graphical methods. The interpolation formulas (47) and (48) are also convenient in the first type of problem in which the wall temperature is calculated from given coolant mass flow.

   Typical examples.- Equations (46), (47), and (48) have been used to calculate the coolant mass flow required to maintain a constant wall temperature in the following three examples:

Example	T_t	T_w	T_c	M_∞
1	10,000	1,500	500	10
2	1,800	800	500	10
3	5,000	1,500	500	7

Examples 1 and 2 represent flight and wind-tunnel conditions, respec-
tively, at $M_\infty \approx 10$. Example 3 represents flight conditions at $M_\infty \approx 7$.
The results are shown in figure 8(a) where the parameter (from eq. (42))

$$\frac{\bar{\omega}}{\left(\frac{\mu_w}{\rho_\infty u_{r,\infty} l} \frac{T_\infty}{T_w}\right)^{1/2}} = -\sqrt{\frac{p_e}{p_\infty} \cos \Lambda \frac{l}{u_\infty} \frac{du_e}{dx}}\, f_w$$

which is directly proportional to the coolant mass flow, is plotted
against yaw angle for $\phi = 1.0$ with $N_{Pr} = 1.0$ and 0.7. Examples 1
and 2 have also been calculated for $\phi \neq 1.0$ with $N_{Pr} = 0.7$ and
s = 0.02. The values used for the velocity-gradient parameter $\left(\frac{l}{u_\infty} \frac{du_e}{dx}\right)$
were taken from reference 21 for a circular cylinder.

Figure 8(a) shows that the coolant mass flow required to maintain a
given temperature decreases with increasing yaw angle, as would be
expected from previous discussion. At small yaw angles considerably more
coolant is required for $N_{Pr} = 0.7$ than for $N_{Pr} = 1.0$; however, the
effect of Prandtl number is not so large for large yaw angles. The
curves calculated for examples 1 and 2 with s = 0.02 indicate that the
use of the Sutherland viscosity relation predicts that less coolant is
required than when the linear viscosity relation is used. The variation
with yaw angle is about the same for both viscosity relations. Note that
in example 1 the curve for $\phi \neq 1.0$, $N_{Pr} = 0.7$ is almost the same as
the curve for $\phi = 1.0$, $N_{Pr} = 1.0$.

In figure 8(b) the corresponding variation of f_w with λ is shown
for these examples. This variation is essentially an effect of compressi-
bility in the boundary layer since for an incompressible boundary layer f_w
would be independent of yaw angle. The present solutions predict, there-
fore, that at large Mach numbers and yaw angles the coolant requirements
would be some 50 percent larger than for an incompressible boundary layer
with the same wall temperature and external flow conditions.

Effect of Pressure Gradient and Yaw-Angle Parameter on

Skin Friction and Heat Transfer

The effects of the pressure-gradient parameter β and the yaw-angle
parameter λ on the heat-transfer and skin-friction parameters for three
different ratios of wall temperature to stream temperature are shown in
figures 9 and 10. These solutions are for the conditions of $\phi = 1.0$,
$N_{Pr} = 1.0$, and $f_w = 0$. The heat-transfer and skin-friction parameters,

as well as other pertinent data from these solutions, are also given in table IV.

Figure 9 indicates that the effects of pressure gradient on the heat-transfer parameter θ_w' or the spanwise skin-friction parameter g_w' (for $N_{Pr} = 1.0$, $\theta_w' = g_w'$) become larger as the wall temperature and yaw parameter are increased. For negative or favorable pressure gradients (positive values of β) the values of θ_w' and g_w' are increased as the yaw parameter λ and the temperature ratio t_w are increased. For adverse pressure gradients, corresponding to negative values of β, the values of θ_w' or g_w' decrease considerably with increasing λ or t_w. For zero pressure gradient, θ_w' or g_w' is independent of both λ and t_w. The effect of these changes on the actual heat transfer or skin friction would have to be calculated from equations (23) or (27) for any given set of flow conditions and wall temperature.

The chordwise skin-friction parameter f_w'' is plotted against β for three wall-temperature ratios and four values of λ in figure 10. The trends shown in figure 10 are the same as those just discussed for θ_w' or g_w'; however, the percentage variations in f_w'' are much larger than in the other parameters. These large variations are particularly noticeable for large values of λ and t_w. The local skin friction must again be calculated for any particular case from the appropriate equations (eq. (26) or (28)).

The value of the pressure-gradient parameter β required for $f_w'' = 0$, implying separation of the chordwise flow, is plotted against λ in figure 11. This figure indicates that decreasing the temperature would delay separation, while increasing the yaw angle (at a sufficiently large stream Mach number) would move separation forward.

The ratio of the chordwise skin-friction parameter to the spanwise skin-friction parameter f_w''/g_w' is indicative of the degree of secondary flow in the boundary layer, as discussed in reference 21. The values of these skin-friction parameters listed in table IV show that the ratio f_w''/g_w' is a maximum for $\beta = 2.0$, unity for a flat plate ($\beta = 0$) where there is no secondary flow, and zero for chordwise separation where the "surface" streamline is exactly in the spanwise direction.

The problem of uniqueness for the solutions with negative β is discussed in appendix C. The particular solutions presented in table IV were obtained by application of the convergence procedure of reference 21

at $\eta = 8$. The tabulated solutions also satisfy the boundary conditions on f' and θ at $\eta = 8$ to within 0.00001 with the absolute values of f'' and $\theta' \leqq 0.00005$. It was found that $f' \leqq 1.00000$ throughout the boundary layer when these conditions were satisfied and that application of the convergence procedure of reference 21 to values of $\eta > 8$ resulted in no appreciable changes in f''_w or θ'_w.

CONCLUDING REMARKS

General equations for the heat transfer and skin friction in the laminar compressible boundary layer on infinite cylinders in yaw are presented for the case in which the velocity and enthalpy profiles are functions of a similarity variable. By means of numerical solutions of the boundary-layer equations, the effects of transpiration cooling, Prandtl number, and viscosity relation were obtained for stagnation-line flow. The effect of chordwise pressure gradient was investigated for a nonporous wall, a Prandtl number of 1.0, and a linear viscosity-temperature relation.

Transpiration cooling reduces the skin-friction and heat-transfer coefficients by large amounts, with the largest percentage reductions occurring at small yaw angles and for a Prandtl number of 1.0. The effect of Prandtl number N_{Pr} on the heat-transfer coefficient is given approximately by $(N_{Pr})^{0.4}$ for a nonporous wall; however, for a porous wall this expression is in considerable error.

Because of an overall reduction in heat-transfer coefficient with yaw angle Λ, the quantity of coolant required to maintain a given wall temperature decreases with increasing Λ; however, this decrease is not so large as that which would be predicted from solutions of the incompressible-boundary-layer equations.

Comparison of solutions computed by using the Sutherland viscosity-temperature relation with solutions computed by using the linear viscosity-temperature relation indicates agreement in heat-transfer coefficients to within about 10 percent when the ratio of wall temperature to stagnation temperature $T_w/T_t \geqq 0.5$. When $T_w/T_t = 0.05$, the heat-transfer coefficients from the two sets of solutions for a cylinder differ by 50 to 150 percent depending on the temperature level and yaw parameter.

The values of the heat-transfer parameter at the stagnation point on a body of revolution obtained by the present method with the Sutherland viscosity-temperature relation and a Prandtl number of 0.7 are in close agreement with the corresponding results of Fay and Riddell for a real gas. This close agreement indicates that the heat-transfer rates at the

stagnation point of a body of revolution or at the stagnation line of a
yawed cylinder in a real-gas flow at equilibrium dissociation may be cal-
culated by using the Sutherland viscosity-temperature relation, the
perfect-gas equation, and constant specific heat in the solution of the
boundary-layer equations. The flow variables appearing in the final
expression for the heat rate must be evaluated at the real-gas conditions.

The effects of pressure gradient on the heat-transfer and skin-
friction parameters become larger as the yaw parameter and wall tempera-
ture are increased. Calculations for an adverse pressure gradient indi-
cate that at sufficiently large values of the stream Mach number the
separation line of the chordwise flow would move forward as the yaw angle
is increased.

Langley Aeronautical Laboratory,
    National Advisory Committee for Aeronautics,
        Langley Field, Va., June 25, 1958.

APPENDIX A

DERIVATION OF SIMPLIFIED BOUNDARY-LAYER EQUATIONS

The equations solved in the present report are essentially the same as the equations of reference 21 except for the boundary condition on the normal velocity at the wall and the assumption used for the viscosity-temperature relation. The normal velocity at the wall is herein assigned a finite value to simulate a porous wall. The injected gas is therefore assumed to be the same as the gas in the boundary layer; that is, the equations apply only for a homogeneous gas throughout. Numerical solutions to the present equations are obtained for both a linear viscosity-temperature relation of the form

$$\mu = \frac{\mu_W}{T_W} T \tag{A1}$$

and for Sutherland's relation

$$\frac{\mu}{\mu_W} = \left(\frac{T}{T_W}\right)^{3/2} \frac{T_W + S}{T + S} \tag{A2}$$

In both equations (A1) and (A2), μ_W would be evaluated as a function of T_W from the best viscosity data available.

Since the basic equations for the compressible boundary layer on the infinite cylinder in yaw are given elsewhere (for example, ref. 21) they are not repeated herein. The assumptions and restrictions used to obtain the following equations are

(1) Prandtl boundary-layer equations for the steady flow of a homogeneous gas

(2) Perfect gas law

$$p = \rho RT \tag{A3}$$

(3) Constant specific heat and Prandtl number

(4) Cylinder of infinite length (spanwise derivatives vanish)

Introducing the stream function and the Stewartson transformation in the same manner as in reference 21 then results in the following system of equations in the transformed coordinate system XZ:

Chordwise momentum equation:

$$\frac{\partial \psi}{\partial Z}\frac{\partial^2 \psi}{\partial X \partial Z} - \frac{\partial \psi}{\partial X}\frac{\partial^2 \psi}{\partial Z^2} = \frac{U_e}{t_s}\frac{dU_e}{dX}\left[\left(1-t_w\right)\theta - \left(1-t_s\right)g^2 + t_w\right] + \nu_t\frac{\partial}{\partial Z}\left(\phi\frac{\partial^2 \psi}{\partial Z^2}\right)$$

(A4)

Spanwise momentum equation:

$$\frac{\partial \psi}{\partial Z}\frac{\partial g}{\partial X} - \frac{\partial \psi}{\partial X}\frac{\partial g}{\partial Z} = \nu_t\frac{\partial}{\partial Z}\left(\phi\frac{\partial g}{\partial Z}\right)$$

(A5)

Energy equation:

$$\frac{\partial \psi}{\partial Z}\frac{\partial \theta}{\partial X} - \frac{\partial \psi}{\partial X}\frac{\partial \theta}{\partial Z} + \frac{1-\theta}{1-t_w}\frac{\partial \psi}{\partial Z}\frac{dt_w}{dX} = \frac{\nu_t}{N_{Pr}}\frac{\partial}{\partial Z}\left\{\phi\left[\frac{\partial \theta}{\partial Z} - \frac{1-N_{Pr}}{1-t_w}\frac{\partial}{\partial Z}\left(\frac{u^2+v^2}{2c_pT_t}\right)\right]\right\}$$

(A6)

The Stewartson transformation used in equations (A4) to (A6) may be defined as

$$\left.\begin{array}{l} X = \displaystyle\int_0^x \frac{\mu_w}{\mu_t}\frac{\rho_w}{\rho_t}\frac{a_e}{a_t}\,dx \\[20pt] Z = \dfrac{a_e}{a_t}\displaystyle\int_0^z \frac{\rho}{\rho_t}\,dz \\[20pt] U = \dfrac{\partial \psi}{\partial Z} \end{array}\right\}$$

(A7)

and the stream function is defined by

$$\frac{\partial \psi}{\partial z} = \frac{\rho}{\rho_t}u$$

$$\frac{\partial \psi}{\partial x} = -\frac{\rho}{\rho_t}w$$

The viscosity function ϕ may be written as

$$\phi = \frac{\mu}{\mu_w} \frac{T_w}{T} \tag{A8}$$

on account of the perfect-gas law and the fact that $\frac{\partial p}{\partial z} = 0$ in a thin boundary layer. In general, T may be expressed as

$$T = T_t \left[\left(1 - t_w\right)\theta - \left(1 - t_s\right)g^2 + t_w - \frac{\gamma - 1}{2} \frac{u_e^2}{a_t^2}\left(\frac{u}{u_e}\right)^2 \right]$$

from the definitions of H, θ, and g and the use of the adiabatic-energy equation for the external flow. The quantity t_s depends on the spanwise velocity and can be written in terms of the stream Mach number and yaw angle as

$$t_s \equiv \frac{1}{\lambda} = 1 - \frac{\gamma - 1}{2}\left(\frac{v_e}{a_t}\right)^2 = \frac{1 + \frac{\gamma - 1}{2} M_\infty^2 \cos^2\Lambda}{1 + \frac{\gamma - 1}{2} M_\infty^2} \tag{A9}$$

which indicates that t_s is simply the ratio of the stagnation temperature of the flow component normal to the cylinder to the total stagnation temperature. Note that the yaw parameter t_s as defined here is the reciprocal of the Mach number—yaw-angle parameter used in reference 21.

Similar solutions to the system of equations (A4) to (A6) are obtained by first assuming that the dimensionless velocity and enthalpy profiles U/U_e, g, and θ are functions of a single similarity variable η and then determining the additional conditions required to reduce the system to ordinary equations (see, for example, ref. 14). The similarity variable is defined as

$$\eta = \sqrt{\frac{m + 1}{2} \frac{U_e}{\nu_t X}} Z \tag{A10}$$

and the assumptions for the profiles are

$$\left. \begin{aligned} \psi &= \sqrt{\frac{2}{m + 1} \nu_t U_e X} f(\eta) \\ g &= g(\eta) \\ \theta &= \theta(\eta) \end{aligned} \right\} \tag{A11}$$

where $U_e = a_t \dfrac{u_e}{a_e}$ and $\dfrac{U}{U_e} = f' = \dfrac{u}{u_e}$. Then, if the external flow is of the Falkner-Skan type

$$U_e = CX^m \tag{A12}$$

the system of equations (A4) to (A6) is reduced to the following form:

$$\frac{\partial}{\partial \eta}\left(\phi f''\right) + f''f = \beta\left\{(f')^2 - \frac{1}{t_s}\left[\left(1 - t_w\right)\theta - \left(1 - t_s\right)g^2 + t_w\right]\right\} \tag{A13}$$

$$\frac{\partial}{\partial \eta}\left(\phi g'\right) + fg' = 0 \tag{A14}$$

$$\frac{\partial}{\partial \eta}(\phi \theta') + N_{Pr}f\theta' - \frac{2N_{Pr}Xf'}{m+1}\frac{1-\theta}{1-t_w}\frac{dt_w}{dX} =$$

$$\frac{1-N_{Pr}}{1-t_w}\frac{\partial}{\partial \eta}\left(\phi\left\{\frac{\gamma-1}{2}\frac{u_e^2}{a_t^2}\left[(f')^2\right]' + \left(1-t_s\right)\left(g^2\right)'\right\}\right) \tag{A15}$$

where the primes denote differentiation with respect to η, and $\beta = \dfrac{2m}{m+1}$. The boundary conditions on equations (A13) to (A15) are now, at $\eta = 0$,

$$f = -w_w\left[\frac{\nu_w}{\beta}\left(1 + \frac{\gamma-1}{2}\frac{u_e^2}{a_e^2}\right)\frac{du_e}{dx}\right]^{-1/2} \tag{A16}$$

where $w_w = 0$ for a nonporous wall and

$$f' = \theta = g = 0 \tag{A17}$$

At $\eta \to \infty$,

$$f' = \theta = g = 1 \tag{A18}$$

For zero aerodynamic heat transfer, the wall temperature in equations (A13) to (A15) is replaced by the adiabatic wall temperature T_{aw}.

Since T_{aw} is then an additional unknown, an additional equation or condition is required in order to evaluate T_{aw}. This additional condition is

$$\left(\frac{\partial \theta}{\partial \eta}\right)_w = 0 \qquad (A19)$$

from the definition of θ. Since t_w and u_e are, in general, functions of X, equations (A13) to (A16) are not yet consistent with the original assumptions for the profiles as given by equations (A11). A consistent set of equations cannot be obtained when t_w is a variable except for incompressible flow $\left(t_w \approx 1.0, \ t_s \approx 1.0, \ u_e \ll a_e\right)$ for which t_w may take the form (see ref. 9)

$$t_w = 1 + AX^n$$

For compressible flow it is necessary to specify that t_w is constant.

While the chordwise velocity U_e must always satisfy equation (A12), the specific value of this velocity required to make equations (A13) to (A16) consistent with equations (A11) depends also on the viscosity assumption and the value of the Prandtl number N_{Pr}. For arbitrary values of ϕ and N_{Pr}, u_e must be either zero (or negligible) or a constant other than zero. The first term on the right in equation (A15) and ϕ then become functions of η only. When u_e is constant, $\beta = 0$, and the equations reduce to the flat-plate case, which is not considered further herein. At $X = 0$, $u_e = 0$ and the equations describe the flow at the stagnation point on a body of revolution (where $\beta = 0.5$ and $t_s = 1.0$) or at the stagnation line on a cylinder ($\beta = 1$). Equations (A13) to (A16) then reduce to

$$(\phi f'')' + f''f = \beta\left\{(f')^2 - \frac{1}{t_s}\left[(1 - t_w)\theta - (1 - t_s)g^2 + t_w\right]\right\} \qquad (A20)$$

$$(\phi g')' + fg' = 0 \qquad (A21)$$

$$(\phi \theta')' + N_{Pr}f\theta' = \left(1 - N_{Pr}\right)\frac{1 - t_s}{1 - t_w}\left[\phi\left(g^2\right)'\right]' \qquad (A22)$$

$$f_w = -w_w\left[\frac{\nu_w}{\beta}\frac{du_e}{dx}\right]^{-1/2} \qquad (A23)$$

with the remaining boundary conditions the same as equations (A17) to
(A19). Equations (A20) to (A23) apply approximately when $u_e \ll a_t$,
which occurs, for example, in the neighborhood of a stagnation line
where $\beta = 1.0$. Small chordwise velocities would also be expected over
the entire cylinder for large yaw angles when the value of β may be
arbitrary. Note that equation (A23) specifies a chordwise distribution
of w_w since f_w must be a constant.

In general, when $u_e \neq 0$, a consistent set of equations can be
obtained only for the condition of $N_{Pr} = 1.0$ and $\phi = 1.0$. The condi-
tion $\phi = 1.0$ is obtained by substituting the linear viscosity relation
given by equation (A1) into equation (A8). The equations (A13) to (A15)
then reduce to

$$f''' + f''f = \beta\left\{(f')^2 - \frac{1}{t_s}\left[\left(1 - t_w\right)\theta - \left(1 - t_s\right)\theta^2 + t_w\right]\right\} \qquad \text{(A24)}$$

$$\theta'' + f\theta' = 0 \qquad \text{(A25)}$$

where for these conditions $\theta = g$, from the boundary conditions (A16) to
(A19) and equation (A14) with $\phi = 1.0$. The boundary conditions applying
to equations (A24) and (A25) are the same as equations (A16) to (A18).
Since f_w must be a constant, the normal velocity at the wall varies
according to

$$w_w = -f_w\left[\frac{\nu_w}{\beta}\left(1 + \frac{\gamma - 1}{2}\frac{u_e^2}{a_e^2}\right)\frac{du_e}{dx}\right]^{1/2}$$

or in terms of the transformed coordinate

$$w_w = -f_w\,\frac{\mu_w}{\mu_t}\,\frac{a_e}{a_t}\,\sqrt{\frac{m + 1}{2}\,\nu_t c x^{m-1}} \qquad \text{(A26)}$$

APPENDIX B

INTEGRAL EQUATIONS IN TRANSFORMED PLANE

A large group of approximate methods for calculating laminar-boundary-layer characteristics are based on the integral equations which are obtained by integrating the partial differential equations across the boundary layer normal to the wall. After suitable assumptions are made for the velocity and temperature profiles, the problem is thereby reduced to the solution of a set of ordinary differential equations. Even though the original boundary-layer equations are satisfied only on the average, these methods are usually considered to be sufficiently accurate for practical purposes. (For a general review of integral methods, see ref. 26.)

Some of the "piecewise" methods (for example, ref. 1) which use basic information from the similar solutions are also found to satisfy the integral momentum or energy equations.

In the application of integral methods to the compressible boundary layer, substantial simplifications are obtained by transforming to the XZ-plane. The velocities in this plane are defined in terms of the stream function ψ as

$$\left.\begin{array}{l} U = \dfrac{\partial \psi}{\partial Z} \\[2em] W = -\dfrac{\partial \psi}{\partial X} \end{array}\right\} \tag{B1}$$

so that the continuity equation is

$$\frac{\partial U}{\partial X} + \frac{\partial W}{\partial Z} = 0 \tag{B2}$$

Substituting equations (B1) into equations (A4) to (A6) of appendix A yields

$$U \frac{\partial U}{\partial X} + W \frac{\partial U}{\partial Z} = \frac{U_e}{t_s} \frac{dU_e}{dX}\left[\left(1 - t_w\right)\theta - \left(1 - t_s\right)g^2 + t_w\right] + \nu_t \frac{\partial}{\partial Z}\left(\phi \frac{\partial U}{\partial Z}\right) \tag{B3}$$

$$U \frac{\partial g}{\partial X} + W \frac{\partial g}{\partial Z} = \nu_t \frac{\partial}{\partial Z}\left(\phi \frac{\partial g}{\partial Z}\right) \tag{B4}$$

$$U \frac{\partial \theta}{\partial X} + W \frac{\partial \theta}{\partial Z} + \frac{1 - \theta}{1 - t_w} U \frac{dt_w}{dX} = \frac{\nu_t}{N_{Pr}} \frac{\partial}{\partial Z}\left(\phi \frac{\partial \theta}{\partial Z}\right) -$$

$$\frac{\nu_t}{N_{Pr}} \frac{1 - N_{Pr}}{1 - t_w} \frac{\partial}{\partial Z}\left[\phi(t_s - t_e)\frac{\partial}{\partial Z}\left(\frac{U^2}{U_e{}^2}\right) + \phi(1 - t_s)\frac{\partial}{\partial Z}(g^2)\right] \tag{B5}$$

where the adiabatic-energy equation for the external flow has been used in the last term of equation (A6). The boundary conditions for equations (B2) to (B5) are, at $Z = 0$,

$$U = \theta = g = 0 \tag{B6}$$

$$W = W_w \tag{B7}$$

where $W_w = 0$ for a nonporous wall; and, at $Z \to \infty$,

$$U = U_e \tag{B8}$$

$$g = \theta = 1 \tag{B9}$$

The conventional boundary-layer assumptions also require that all derivatives of U, g, and θ become negligible for large values of Z. For zero heat transfer the additional condition $(\partial\theta/\partial Z)_w = 0$ is used to determine the adiabatic wall temperature T_{aw}. Combining equations (B2) and (B3) and integrating from $Z = 0$ to ∞ with boundary conditions (B6) to (B9) then yield

$$\frac{d}{dX} \int_0^\infty \left(\frac{U}{U_e} - \frac{U^2}{U_e{}^2}\right)dZ - \frac{W_w}{U_e} + \frac{1}{U_e}\frac{dU_e}{dX}\left\{ 2 \int_0^\infty \left(\frac{U}{U_e} - \frac{U^2}{U_e{}^2}\right)dZ + \int_0^\infty \left(1 - \frac{U}{U_e}\right)dZ + \right.$$

$$\left. \frac{1}{t_s}\left[(1 - t_s) \int_0^\infty (1 - g^2)dZ + (t_w - 1) \int_0^\infty (1 - \theta)dZ\right]\right\} = \frac{\nu_t}{U_e}\left(\frac{\partial}{\partial Z}\frac{U}{U_e}\right)_w \tag{B10}$$

Equations (B2) and (B4) can be combined in the same manner to give

$$\frac{d}{dX} \int_0^\infty \frac{U}{U_e}(1 - g)dZ - \frac{W_w}{U_e} + \frac{1}{U_e}\frac{dU_e}{dX} \int_0^\infty \frac{U}{U_e}(1 - g)dZ = \frac{\nu_t}{U_e}\left(\frac{\partial g}{\partial Z}\right)_w \tag{B11}$$

Similarily, equations (B2) and (B5) yield

$$\frac{d}{dX} \int_0^\infty \frac{U}{U_e}(1 - \theta)dZ - \frac{W_w}{U_e} + \frac{1}{U_e}\frac{dU_e}{dX} \int_0^\infty \frac{U}{U_e}(1 - \theta)dZ -$$

$$\frac{1}{1 - t_w}\frac{dt_w}{dX} \int_0^\infty \frac{U}{U_e}(1 - \theta)dZ = \frac{\nu_t}{N_{Pr}U_e}\left(\frac{\partial \theta}{\partial Z}\right)_w \tag{B12}$$

The integral-thickness parameters are defined as follows:

$$\left.\begin{aligned}
\theta^* &= \int_0^\infty \left(\frac{U}{U_e} - \frac{U^2}{U_e{}^2}\right)dZ \\[2mm]
\delta^* &= \int_0^\infty \left(1 - \frac{U}{U_e}\right)dZ \\[2mm]
G &= \int_0^\infty \left(1 - g^2\right)dZ \\[2mm]
E &= \int_0^\infty \frac{U}{U_e}(1 - g)dZ \\[2mm]
\Theta &= \int_0^\infty \frac{U}{U_e}(1 - \theta)dZ \\[2mm]
\Theta^* &= \int_0^\infty (1 - \theta)dZ
\end{aligned}\right\} \tag{B13}$$

Substitution of these parameters into equations (B10) to (B12) then gives the final form of the integral equations as

$$\frac{d\theta^*}{dX} + \frac{1}{U_e}\frac{dU_e}{dX}\left\{2\theta^* + \delta^* + \frac{1}{t_s}\left[(1 - t_s)G + (t_w - 1)\Theta^*\right]\right\} = \frac{\nu_t}{U_e}\left(\frac{\partial}{\partial Z}\frac{U}{U_e}\right)_w + \frac{W_w}{U_e}$$

<div align="right">(B14)</div>

$$\frac{dE}{dX} + \frac{E}{U_e}\frac{dU_e}{dX} = \frac{\nu_t}{U_e}\left(\frac{\partial g}{\partial Z}\right)_w + \frac{W_w}{U_e} \tag{B15}$$

$$\frac{d\Theta}{dX} + \Theta\left(\frac{1}{U_e}\frac{dU_e}{dX} - \frac{1}{1 - t_w}\frac{dt_w}{dX}\right) = \frac{\nu_t}{N_{Pr}U_e}\left(\frac{\partial\theta}{\partial Z}\right)_w + \frac{W_w}{U_e} \tag{B16}$$

The normal velocity at the wall in the transformed plane is related to the corresponding velocity in the physical plane by the relation

$$W_w = \frac{\mu_t}{\mu_w}\frac{a_t}{a_e}w_w$$

from equations (A7) and the definitions of U and W.

APPENDIX C

UNIQUENESS OF SOLUTIONS FOR NEGATIVE VALUES OF β

In order to discuss the uniqueness problem for negative values of β (see refs. 4, 5, and 14) it is useful to consider the asymptotic solutions to equations (A24) and (A25). These equations apply for $\emptyset = 1.0$ and $N_{Pr} = 1.0$ and are as follows:

$$f''' + f''f = \beta \left\{ (f')^2 - \frac{1}{t_s} \left[(1 - t_w)\theta - (1 - t_s)\theta^2 + t_w \right] \right\} \qquad (C1)$$

$$\theta'' + f\theta' = 0 \qquad (C2)$$

The boundary conditions are, at $\eta = 0$,

$$f = f_w \qquad (C3)$$

$$f' = \theta = 0 \qquad (C4)$$

and, at $\eta \to \infty$,

$$f' = \theta = 1.0 \qquad (C5)$$

The functions f' and θ may be written as

$$\left. \begin{aligned} f' &= 1 - \bar{f} \\ \theta &= 1 - \bar{\theta} \end{aligned} \right\} \qquad (C6)$$

where, at large values of η, $\bar{f}$ and $\bar{\theta}$ are small quantities because of boundary conditions (C3) to (C5). Substituting equations (C6) into equations (C1) and (C2) and retaining only the linear terms in $\bar{f}$ and $\bar{\theta}$ result in the equations

$$\bar{f}'' + \bar{f}'f = 2\beta\bar{f} + \beta\bar{\theta}\left(\frac{1 + t_w}{t_s} - 2\right) \qquad (C7)$$

$$\bar{\theta}'' + f\bar{\theta}' = 0 \qquad (C8)$$

which are valid only at large values of η. The boundary conditions
for $\eta \rightarrow \infty$ are now

$$\bar{f} = 0$$

$$\bar{\theta} = 0$$

The function f may be written by definition as

$$f = f_e + \int_{\eta_e}^{\eta} f' d\eta$$

which, from equations (C6), becomes

$$f = f_e + \int_{\eta_e}^{\eta} (1 - \bar{f}) d\eta$$

If the quantity $\displaystyle\int_{\eta_e}^{\infty} \bar{f} \, d\eta$ is assumed to be negligible, the asymptotic
expression for f is

$$f = f_e + \eta - \eta_e \tag{C9}$$

Introducing the variable $\bar{\eta}$ defined as

$$\bar{\eta} = \eta + \left(f_e - \eta_e\right) \tag{C10}$$

and substituting equation (C9) into equations (C7) and (C8) then result
in

$$\frac{d^2\bar{f}}{d\bar{\eta}^2} + \bar{\eta} \frac{d\bar{f}}{d\bar{\eta}} = 2\beta\bar{f} + \beta\bar{\theta}\left(\frac{1 + t_w}{t_s} - 2\right) \tag{C11}$$

$$\frac{d^2\bar{\theta}}{d\bar{\eta}^2} + \bar{\eta} \frac{d\bar{\theta}}{d\bar{\eta}} = 0 \tag{C12}$$

The required solution to equation (C12) is

$$\bar{\theta} = \theta_e' e^{\frac{1}{2}f_e^2} \int_{\bar{\eta}}^{\infty} e^{-\frac{1}{2}\bar{\eta}^2} \, d\bar{\eta}$$

since from equation (C10) $\bar{\eta}_e = f_e$. For large values of $\bar{\eta}$ this relation may be expressed as (see ref. 27)

$$\bar{\theta} = \theta_e' \frac{e^{\frac{1}{2}\left(f_e^2 - \bar{\eta}^2\right)}}{\bar{\eta}} \tag{C13}$$

Thus at $\eta = \eta_e$, where η_e is such that (C9) is satisfied, the asymptotic solution for θ as given by equation (C13) requires that approximately

$$\theta_e \approx 1 - \frac{\theta_e'}{f_e} \tag{C14}$$

which may be verified for $\beta = 1.0$ from the tabulated results for $N_{Pr} = 1.0$ in reference 21.

Substituting equation (C13) into equation (C11) results in the linear differential equation

$$\frac{d^2\bar{f}}{d\bar{\eta}^2} + \bar{\eta}\frac{d\bar{f}}{d\bar{\eta}} - 2\beta\bar{f} = \beta\left(\frac{1+t_w}{t_s} - 2\right)\theta_e' \frac{e^{\frac{1}{2}\left(f_e^2 - \bar{\eta}^2\right)}}{\bar{\eta}} \tag{C15}$$

A particular integral of this equation valid for large values of $\bar{\eta}$ is

$$\bar{f} = A \frac{e^{-\frac{1}{2}\bar{\eta}^2}}{\bar{\eta}} \tag{C16}$$

where, by substitution in equation (C15),

$$A = -\frac{1}{2}\left(\frac{1+t_w}{t_s} - 2\right)\theta_e' e^{\frac{1}{2}f_e^2} \tag{C17}$$

The general solution to the homogeneous part of equation (C15) for large values of η is (see ref. 4)

$$\bar{f} = \frac{B}{\bar{\eta}^{(2\beta+1)} e^{\frac{1}{2}\bar{\eta}^2}} + K\eta^{2\beta} \tag{C18}$$

where for $\beta > 0$, $K = 0$ in order to satisfy the boundary condition $\bar{f} = 0$ for $\eta \to \infty$.

For $\beta < 0$ this boundary condition can be satisfied with any finite value of K and the general solution to equation (C15) then becomes

$$\bar{f} = \frac{1}{e^{\frac{1}{2}\bar{\eta}^2}}\left[\left(1 - \frac{1 + t_w}{2t_s}\right)\theta_e' \frac{e^{\frac{1}{2}f_e^2}}{\bar{\eta}} + \frac{B}{\bar{\eta}^{(2\beta+1)}}\right] + K\bar{\eta}^{2\beta} \qquad (C19)$$

which is valid only for large values of $\bar{\eta}$ and $\beta < 0$. Since equation (C19) is a solution for any value of K, further restrictions must be imposed before a unique solution can be obtained. Hartree (ref. 4) sets $K = 0$ for reasons of continuity and consistency with the $\beta > 0$ case. Cohen and Reshotko (ref. 14) state further that for $\beta < 0$ it is necessary to set $K = 0$ to avoid infinite displacement thickness. For $K = 0$ the constant B may be obtained from equation (C19) evaluated at $\bar{\eta} = \bar{\eta}_e$. The final asymptotic forms for f' and θ may then be written as

$$f' = 1 - \frac{1}{e^{\frac{1}{2}\left(\bar{\eta}^2 - f_e^2\right)}} \frac{f_e}{\bar{\eta}}\left\{\left(1 - \frac{1 + t_w}{2t_s}\right)\frac{\theta_e'}{f_e} + \left(\frac{f_e}{\bar{\eta}}\right)^{2\beta}\left[1 - f_e' - \left(1 - \frac{1 + t_w}{2t_s}\right)\frac{\theta_e'}{f_e}\right]\right\}$$

$$(C20)$$

$$\theta = 1 - \frac{1}{e^{\frac{1}{2}\left(\bar{\eta}^2 - f_e^2\right)}} \frac{\theta_e'}{\bar{\eta}} \qquad (C21)$$

Equations (C20) and (C21) are now unique solutions for all values of β, and a study of their properties for $\beta < 0$ may be used as a guide to obtain by numerical methods the corresponding unique solutions of the original nonlinear differential equations (A24) and (A25).

For purposes of comparison, consider first the cases for $\beta > 0$ and $\beta = 0$. For $\beta > 0$ the first term in the braces of equation (C20) dominates so that for very large values of $\bar{\eta}$ there remains approximately

$$f' \approx 1 - \frac{1}{e^{\frac{1}{2}\left(\bar{\eta}^2 - f_e^2\right)}} \frac{\theta_e'}{\bar{\eta}}\left(1 - \frac{1 + t_w}{2t_s}\right)$$

Hence for $\theta_e' > 0$, $f' \rightarrow 1$ from above or below according to whether $\frac{1 + t_w}{2t_s}$ is greater or less than 1.0. All numerical solutions (whether

unique or not) obtained in the present investigation for $N_{Pr} = 1.0$
show that $\theta_e' \gtreqless 0$ for both negative and positive values of β. The
asymptotic solutions for $\beta = 1.0$ are discussed in detail in reference 21.

For $\beta = 0$, equation (C20) reduces to

$$f' = 1 - \frac{1}{e^{\frac{1}{2}\left(\bar{\eta}^2 - f_e^2\right)}} \frac{f_e}{\bar{\eta}}\left(1 - f_e'\right)$$

which shows that for $f_e' < 1.0$, $f' \to 1$ from below.

For $\beta < 0$, the second term in the braces of equation (C20) dominates
so that for very large values of $\bar{\eta}$

$$f' \approx 1 - \frac{1}{e^{\frac{1}{2}\left(\bar{\eta}^2 - f_e^2\right)}}\left(\frac{f_e}{\bar{\eta}}\right)^{2\beta+1}\left[1 - f_e' - \left(1 - \frac{1 + t_w}{2t_s}\right)\frac{\theta_e'}{f_e}\right]$$

which shows that $f' \to 1.0$ from below if

$$\left(1 - f_e'\right) > \left(1 - \frac{1 + t_w}{2t_s}\right)\frac{\theta_e'}{f_e} \tag{C22}$$

This inequality would always be satisfied for $\theta_e' > 0$ and $f_e' < 1$ if
$\frac{1 + t_w}{2t_s} \gtreqless 1$. On the other hand $f' \to 1.0$ from above if

$$\left(1 - f_e'\right) < \left(1 - \frac{1 + t_w}{2t_s}\right)\frac{\theta_e'}{f_e} \tag{C23}$$

which is always satisfied for $\theta_e' > 0$ and $f_e' > 1$ if
$\frac{1 + t_w}{2t_s} \equiv \frac{1 + t_w}{2}\lambda \leqq 1.0$. Apparently a unique solution is possible when
velocity overshoot $\left(f_e' > 1\right)$ occurs if $\frac{1 + t_w}{2}\lambda \leqq 1.0$ and equation (C21),
as well as all boundary conditions, is also satisfied. (The situation
for negative values of β, or adverse pressure gradient, is the exact
opposite of that at positive values of β, or favorable pressure gradient,
where velocity overshoot occurred for $\frac{1 + t_w}{2}\lambda > 1.0$.) In the present

solutions for negative values of β the smallest value of $\frac{1 + t_w}{2} \lambda$ is 0.8, a value corresponding to $t_w = 0$ and $\lambda = 1.6$. (Solutions for $\lambda = 1.0$ are given in ref. 14.) If a valid solution with velocity overshoot is possible, it would be expected for these values of t_w and λ. A series of solutions were then obtained for $t_w = 0$, $\lambda = 1.6$, and $\beta = -0.2$ for different values of η, say η^*, at which the convergence procedure as described in reference 21 was applied. Pertinent values from these solutions are presented in table VI. Examination of the tabulated values of $\left(1 - f'_e\right)$ and $\left(1 - \frac{1 + t_w}{2} \lambda\right)\frac{\theta'_e}{f_e} = 0.2 \frac{\theta'_e}{f_e}$ shows that when inequality (C23) is satisfied the boundary conditions on f' and θ at large values of η are not satisfied. Furthermore, equation (C21) is not satisfied since θ'_e always remains positive even when $\theta > 1.0$.

The boundary condition on θ was not satisfied to a high degree of accuracy until $f'_e \leqq 1.0$ for all values of η whereupon the inequality (C22) was satisfied at $\eta = 6$ and 8. It is therefore concluded that for the particular convergence procedure used herein it is not possible to satisfy equations (C20) and (C21) simultaneously when $\frac{1 + t_w}{2} \lambda \leqq 1.0$ and velocity overshoot occurs. In other words, while equation (C18) permits a unique solution with velocity overshoot, the required boundary conditions on θ and θ' cannot be obtained when velocity overshoot is present.

The results shown in table VI also indicate that increasing η^* from 6.8 to 10.4 resulted in no change in f''_w and θ'_w and very little change in any of the tabulated values at comparable values of η. The same behavior was noted in several other sets of solutions at different values of t_w, λ, and negative β.

In view of the preceding discussion concerning the asymptotic solution and also because of the tendency for f''_w and θ'_w to approach constant values as η^* is increased, it was assumed that, in general, unique solutions could be obtained by using $\eta^* = 8.0$ provided that $f' \leqq 1$ for all values of η and the boundary conditions at $\eta = 8.0$ were satisfied to within 0.00001 on θ and f', and to within 0.00005 on θ' and f''. All final solutions for negative values of β as presented in table IV satisfy these conditions to this degree of accuracy.

REFERENCES

1. Eckert, E. R. G., and Livingood, John N. B.: Method for Calculation of Laminar Heat Transfer in Air Flow Around Cylinders of Arbitrary Cross Section (Including Large Temperature Differences and Transpiration Cooling). NACA Rep. 1118, 1953. (Supersedes NACA TN 2733.)

2. Smith, A. M. O.: Rapid Laminar Boundary-Layer Calculations by Piecewise Application of Similar Solutions. Jour. Aero. Sci., vol. 23, no. 10, Oct. 1956, pp. 901-912.

3. Stine, Howard A., and Wanlass, Kent: Theoretical and Experimental Investigation of Aerodynamic-Heating and Isothermal Heat-Transfer Parameters on a Hemispherical Nose With Laminar Boundary Layer at Supersonic Mach Numbers. NACA TN 3344, 1954.

4. Hartree, D. R.: On an Equation Occurring in Falkner and Skan's Approximate Treatment of the Equations of the Boundary Layer. Proc. Cambridge Phil. Soc., vol. XXXIII, pt. 2, Apr. 1937, pp. 223-239.

5. Smith, A. M. O.: Improved Solutions of the Falkner and Skan Boundary-Layer Equation. Rep. No. ES 16009 (Contract No. NOa(s)9027), Douglas Aircraft Co., Inc., Mar. 31, 1952.

6. Fluid Motion Panel of the Aeronautical Research Committee and Others: Modern Developments in Fluid Dynamics. Vol. II, ch. XIV, sec. 270, S. Goldstein, ed., The Clarendon Press (Oxford), 1938, p. 631.

7. Sibulkin, M.: Heat Transfer Near the Forward Stagnation Point of a Body of Revolution. Jour. Aero. Sci. (Readers' Forum), vol. 19, no. 8, Aug. 1952, pp. 570-571.

8. Schuh, H.: Laminar Heat Transfer in Boundary Layers at High Velocities. Reps. and Translations No. 810, British M.A.P. Völkenrode, Apr. 15, 1947.

9. Levy, Solomon: Heat Transfer to Constant-Property Laminar Boundary-Layer Flows With Power-Function Free-Stream Velocity and Wall-Temperature Variation. Jour. Aero. Sci., vol. 19, no. 5, May 1952, pp. 341-348.

10. Donoughe, Patrick L., and Livingood, John N. B.: Exact Solutions of Laminar-Boundary-Layer Equations With Constant Property Values for Porous Wall With Variable Temperature. NACA Rep. 1229, 1955. (Supersedes NACA TN 3151.)

11. Brown, W. Byron, and Donoughe, Patrick L.: Tables of Exact Laminar-Boundary-Layer Solutions When the Wall Is Porous and Fluid Properties Are Variable. NACA TN 2479, 1951.

12. Brown, W. Byron, and Livingood, John N. B.: Solutions of Laminar-Boundary-Layer Equations Which Result in Specific-Weight-Flow Profiles Locally Exceeding Free-Stream Values. NACA TN 2800, 1952.

13. Levy, Solomon: Effect of Large Temperature Changes (Including Viscous Heating) Upon Laminar Boundary Layers With Variable Free-Stream Velocity. Jour. Aero. Sci., vol. 21, no. 7, July 1954, pp. 459-474.

14. Cohen, Clarence B., and Reshotko, Eli: Similar Solutions for the Compressible Laminar Boundary Layer With Heat Transfer and Pressure Gradient. NACA Rep. 1293, 1956. (Supersedes NACA TN 3325.)

15. Reshotko, Eli, and Cohen, Clarence B.: Heat Transfer at the Forward Stagnation Point of Blunt Bodies. NACA TN 3513, 1955.

16. Cooke, J. C.: The Boundary Layer of a Class of Infinite Yawed Cylinders. Proc. Cambridge Phil. Soc., vol. 46, pt. 4, Oct. 1950, pp. 645-648.

17. Crabtree, L. F.: The Compressible Laminar Boundary Layer on a Yawed Infinite Wing. Aero. Quarterly, vol. V, pt. 2, July 1954, pp. 85-100.

18. Moore, Franklin K.: Three-Dimensional Boundary Layer Theory. Vol. IV of Advances in Applied Mechanics, H. L. Dryden and Th. von Kármán, eds., Academic Press, Inc. (New York), 1956, pp. 159-228.

19. Tinkler, J.: Effect of Yaw on the Compressible Laminar Boundary Layer. R. & M. No. 3005, British A.R.C., 1957.

20. Lew, H. G., and Fanucci, J. B.: Effect of Yaw on Boundary Layers at High Speeds. Tech. Rep. No. 9 (Contract No. AF 18(600)-575), Dept. Aero. Eng., The Pennsylvania State Univ., Nov. 1956. (Also available as AF OSR-TN-57-221, ASTIA Doc. AD-126519.)

21. Reshotko, Eli, and Beckwith, Ivan E.: Compressible Laminar Boundary Layer Over a Yawed Infinite Cylinder With Heat Transfer and Arbitrary Prandtl Number. NACA TN 3986, 1957.

22. Lew, H. G., and Fanucci, J. B.: Heat Transfer and Skin Friction of Yawed Infinite Wings With Large Suction. Tech. Rep. No. 8 (Contract No. AF 18(600)-575), Dept. Aero. Eng., The Pennsylvania State Univ., Nov. 1956. (Also available as AF OSR-TN-57-63, ASTIA Doc. AD-120404.)

23. Fay, J. A., and Riddell, F. R.: Theory of Stagnation Point Heat
    Transfer in Dissociated Air. Jour. Aero. Sci., vol. 25, no. 2,
    Feb. 1958, pp. 73-85,121.

24. Moore, Franklin K.: Displacement Effect of a Three-Dimensional
    Boundary Layer. NACA Rep. 1124, 1953. (Supersedes NACA TN 2722.)

25. Gill, S.: A Process for the Step-by-Step Integration of Differential
    Equations in an Automatic Digital Computing Machine. Proc. Cambridge
    Phil. Soc., vol. 47, pt. 1, Jan. 1951, pp. 96-108.

26. Morduchow, Morris: Analysis and Calculation by Integral Methods of
    Laminar Compressible Boundary Layer With Heat Transfer and With
    and Without Pressure Gradient. NACA Rep. 1245, 1955.

27. Feller, William: An Introduction to Probability Theory and Its
    Applications. Vol. 1, John Wiley & Sons, Inc., c.1950, pp. 129-131.

TABLE I

BOUNDARY-LAYER PARAMETERS CALCULATED AT STAGNATION LINE OF A YAWED

CYLINDER BY USING LINEAR VISCOSITY-TEMPERATURE RELATION

$N_{Pr} = 1.0$

f_w	t_w	λ	f_w''	θ_w' or g_w'	δ_{tr}^*	G_{tr}	θ_{tr}^*	θ_{tr}^*
0	0	1.0	0.6489	0.5067	0.9793	1.5792	1.1371	0.4033
		1.6	.7475	.5248	.8667	1.5311	1.1015	.3623
		3.0	.9607	.5603	.6543	1.4451	1.0381	.2652
		6.5	1.4313	.6254	.2834	1.3089	.9381	.0233
	.5	1.0	.9548	.5421	.7929	1.4933	1.0730	.3492
		1.6	1.2062	.5728	.6230	1.4236	1.0214	.2731
		3.0	1.7341	.6280	.3302	1.3124	.9396	.0942
		6.5	2.8663	.7213	-.1346	1.1581	.8269	-.3407
	1.0	1.0	1.2326	.5705	.6479	1.4305	1.0262	.2923
		1.6	1.6149	.6094	.4437	1.3503	.9671	.1805
		3.0	2.4086	.6770	.1053	1.2298	.8787	-.0781
		6.5	4.0951	.7871	-.4106	1.0720	.7640	-.6952
-0.5	0	1.0	0.3067	0.2031	1.4844	2.3271	1.7562	0.5392
		1.6	.3910	.2261	1.2580	2.1854	1.6420	.4745
		3.0	.5718	.2678	.8873	1.9705	1.4706	.3278
		6.5	.9720	.3392	.3369	1.6898	1.2504	-.0155
	.5	1.0	.6669	.2580	1.0437	2.0350	1.5191	.4414
		1.6	.9145	.2945	.7619	1.8751	1.3924	.3208
		3.0	1.4258	.3558	.3346	1.6571	1.2219	.0549
		6.5	2.5128	.4537	-.2630	1.3986	1.0231	-.5458
	1.0	1.0	.9692	.2950	.7809	1.8781	1.3940	.3441
		1.6	1.3492	.3390	.4752	1.7171	1.2677	.1719
		3.0	2.1285	.4115	.0209	1.5053	1.1039	-.2015
		6.5	3.7747	.5249	-.6052	1.2622	.9187	-1.0311
-1.0	0	1.0	0.0474	0.0211	3.0611	4.2746	3.5535	0.7699
		1.6	.0970	.0371	2.2986	3.6041	2.9335	.6648
		3.0	.2159	.0699	1.4472	2.9185	2.3194	.4449
		6.5	.5070	.1298	.5233	2.2765	1.7660	-.0289
	.5	1.0	.4519	.0823	1.4181	2.8171	2.2178	.5713
		1.6	.6740	.1126	.9575	2.4836	1.9309	.3855
		3.0	1.1390	.1652	.3491	2.0915	1.6016	.0046
		6.5	2.1447	.2520	-.4038	1.6851	1.2699	-.7962
	1.0	1.0	.7566	.1168	.9449	2.4587	1.9075	.4058
		1.6	1.1117	.1546	.5068	2.1704	1.6650	.1513
		3.0	1.8467	.2184	-.0817	1.8304	1.3855	-.3662
		6.5	3.4163	.3213	-.8236	1.4780	1.1032	-1.4446

$N_{Pr} = 0.7$

f_w	t_w	λ	f_w''	g_w'	θ_w'	$\bar{h}$	δ_{tr}^*	G_{tr}	θ_{tr}^*	θ_{tr}^*
0	0	1.0	0.6071	0.4970	0.4362	0.4362	1.0560	1.6075	1.3240	0.4376
		1.6	.6870	.5129	.4226	.4475	.9507	1.5635	1.2507	.3996
		3.0	.8617	.5444	.4262	.4712	.7465	1.4823	1.1563	.3097
		6.5	1.2526	.6041	.4582	.5184	.3776	1.3489	1.0324	.0833
	.5	1.0	.9362	.5382	.4696	.4696	.8241	1.5036	1.2435	.3669
		1.6	1.1824	.5692	.4386	.4935	.6429	1.4316	1.1070	.2831
		3.0	1.7009	.6252	.4350	.5377	.3279	1.3165	.9542	.0856
		6.5	2.8164	.7200	.4717	.6145	-.1758	1.1574	.7935	-.3974
	1.0	1.0	1.2326	.5705	0		.6479	1.4305	.4793	.2923
	.9444	1.6	1.5724	.6067	0		.4450	1.3544	.4021	.1753
	.9045	3.0	2.2902	.6716	0		.0969	1.2361	.2906	-.0978
	.8838	6.5	3.8392	.7797	0		-.4502	1.0771	.1602	-.7569
-0.5	0	1.0	0.2966	0.1985	0.2103	0.2103	1.5567	2.3626	1.9052	0.5725
		1.6	.3639	.2177	.2087	.2248	1.3542	2.2376	1.7883	.5143
		3.0	.5105	.2540	.2229	.2536	1.0057	2.0370	1.6106	.3813
		6.5	.8401	.3186	.2627	.3067	.4601	1.7594	1.3732	.0644
	.5	1.0	.6610	.2560	.2600	.2600	1.0726	2.0470	1.6601	.4592
		1.6	.8999	.2914	.2469	.2884	.7859	1.8880	1.4827	.3337
		3.0	1.3962	.3521	.2560	.3379	.3411	1.6674	1.2571	.0530
		6.5	2.4575	.4502	.2990	.4191	-.2938	1.4031	1.0108	-.5904
	1.0	1.0	.9692	.2950	0		.7809	1.8781	1.1596	.3441
	.9280	1.6	1.2850	.3332	0		.4992	1.7349	1.0042	.1803
	.8789	3.0	2.1356	.3999	0		.0501	1.5316	.7883	-.1859
	.8566	6.5	3.4115	.5090	0		-.6032	1.2856	.5429	-1.0250
-1.0	0	1.0	0.0705	0.0276	0.0496	0.0496	2.7818	3.9909	3.2712	0.7800
		1.6	.1120	.0400	.0579	.0634	2.2520	3.5413	2.9003	.6879
		3.0	.2101	.0666	.0783	.0916	1.5350	2.9773	2.4200	.4902
		6.5	.4500	.1183	.1180	.1422	.6552	2.3714	1.9011	.0546
	.5	1.0	.4551	.0825	.1112	.1112	1.4290	2.8174	2.2846	.5842
		1.6	.6700	.1114	.1148	.1390	.9784	2.4968	2.0042	.3984
		3.0	1.1211	.1624	.1321	.1864	.3614	2.1078	1.6498	.0094
		6.5	2.0998	.2481	.1738	.2634	-.4255	1.6961	1.2773	-.8260
		6.5	^{a}2.0999	^{a}.2481	^{a}.1738					
	1.0	1.0	.7566	.1168	0		.9450	2.4589	1.8625	.4058
	.9128	1.6	1.0342	.1475	0		.5650	2.2151	1.6075	.1822
	.8544	3.0	1.6355	.2036	0		-.0018	1.8924	1.2725	-.2959
	.8299	6.5	2.9719	.2996	0		-.7706	1.5313	.9046	-1.3397

$^a \Delta\eta = 0.1$.

TABLE II

BOUNDARY-LAYER PARAMETERS CALCULATED AT STAGNATION LINE OF A YAWED CYLINDER BY USING

SUTHERLAND VISCOSITY-TEMPERATURE RELATION AND PRANDTL NUMBER OF 0.7

s = 0.2

f_w	t_w	λ	f''_w	g'_w	θ'_w	$\bar{h}$	ϕ_∞	δ^*_{tr}	G_{tr}	θ^*_{tr}	$\bar{\theta}^*_{tr}$
0	0.05	1.0	0.6891	0.5347	0.4661	0.4661	0.9317	1.1244	1.7259	1.4278	0.4605
		1.6	.8095	.5656	.4634	.4927	1.0714	.9998	1.6871	1.3501	.4248
		3.0	1.0547	.6132	.4768	.5322	1.2103	.7565	1.6030	1.2445	.3196
		6.5	1.5840	.6894	.5188	.5947	1.2393	.3221	1.4553	1.1043	.0384
		11.0	2.1821	.7569	.5636	.6506	1.1588	-.0581	1.3361	1.0038	-.3156
0	.5	1.0	.9109	.5158	.4484	.4484	.8250	.8105	1.4596	1.2119	.3532
		1.6	1.1641	.5563	.4286	.4832	.9486	.6370	1.4066	1.0904	.2777
		3.0	1.6857	.6205	.4311	.5372	1.0716	.3237	1.3092	.9468	.0819
		6.5	2.7976	.7204	.4702	.6207	1.0973	-.1899	1.1608	.7904	-.4139
		11.0	4.0350	.8047	.5158	.6913	1.0260	-.6139	1.0520	.6957	-1.0223
0	1.0	1.0	1.2326	.5705	0		1.0	.6479	1.4305	.4789	.2923
	.9435	1.6	1.5771	.6143	0		1.1281	.4436	1.3688	.4024	.1743
	.9012	3.0	2.2956	.6865	0		1.2557	.0819	1.2637	.2899	-.1139
	.8787	6.5	3.8408	.8010	0		1.2756	-.5026	1.1114	.1561	-.8230
	.8730	11.0	5.5679	.8979	0		1.1903	-.9819	1.0029	.0809	-1.6832
-0.5	0.05	1.0	0.3858	0.2391	0.2452	0.2452		1.5820	2.4425	1.9830	0.5938
		1.6	.4925	.2713	.2521	.2730		1.3456	2.3065	1.8441	.5330
		3.0	.7101	.3221	.2746	.3158		.9564	2.1003	1.6510	.3792
		6.5	1.1805	.4029	.3238	.3837		.3560	1.8190	1.4054	-.0008
		11.0	1.7151	.4729	.3717	.4427		-.1215	1.6233	1.2423	-.4574
-0.5	.5	1.0	.6430	.2386	.2430	.2430		1.0680	2.0167	1.6442	.4486
		1.6	.8860	.2807	.2384	.2790		.7832	1.8682	1.4716	.3296
		3.0	1.3833	.3472	.2522	.3355		.3382	1.6613	1.2513	.0497
		6.5	2.4399	.4492	.2969	.4220		-.3072	1.4068	1.0084	-.6064
		11.0	3.6174	.5341	.3435	.4941		-.8018	1.2426	.8656	-1.3730
-0.5	1.0	1.0	.9692	.2950	0			.7809	1.8781	1.1596	.3441
	.9271	1.6	1.2868	.3382	0			.4977	1.7464	1.0029	.1791
	.8759	3.0	1.9549	.4102	0			.0368	1.5559	.7876	-.2002
	.8519	6.5	3.4045	.5247	0			-.6514	1.3172	.5410	-1.0840
	.8476	11.0	5.0371	.6212	0			-1.1875	1.1628	.3987	-2.1174
-1.0	0.05	1.0	0.1572	0.0553	0.0819	0.0819		2.4491	3.7002	3.0163	0.7867
		1.6	.2368	.0786	.0968	.1067		1.9551	3.3077	2.6822	.6870
		3.0	.4075	.1194	.1243	.1474		1.2890	2.8303	2.2697	.4633
		6.5	.7934	.1892	.1737	.2128		.4377	2.3058	1.8210	-.0406
		11.0	1.2465	.2521	.2194	.2700		-.1678	1.9900	1.5548	-.6186
-1.0	.5	1.0	.4458	.0740	.1010	.1010		1.4353	2.8048	2.2907	.5779
		1.6	.6616	.1051	.1092	.1325		.9799	2.4845	2.0016	.3961
		3.0	1.1118	.1585	.1291	.1836		.3603	2.1041	1.6469	.0068
		6.5	2.0855	.2463	.1717	.2640		-.4380	1.7006	1.2761	-.8410
		11.0	3.1845	.3225	.2139	.3320		-1.0077	1.4644	1.0687	-1.7872
-1.0	1.0	1.0	.7566	.1168	0			.9450	2.4589	1.8625	.4058
	.9118	1.6	1.0343	.1499	0			.5638	2.2246	1.6074	.1811
	.8514	3.0	1.6325	.2092	0			-.0130	1.9140	1.2731	-.3077
	.8253	6.5	2.9609	.3095	0			-.8140	1.5607	.9059	-1.3901
	.8222	11.0	4.4810	.3973	0			-1.4089	1.3480	.6964	-2.6140

s = 0.02

f_w	t_w	λ	f''_w	g'_w	θ'_w	$\bar{h}$	ϕ_∞	δ^*_{tr}	G_{tr}	θ^*_{tr}	$\bar{\theta}^*_{tr}$
0	0.05	1.0	0.4576	0.3444	0.2969	0.2969	0.3069	0.8627	1.2475	1.0566	0.2993
		1.6	.5551	.3743	.3046	.3241	.3837	.7835	1.2332	1.0139	.2864
		3.0	.7498	.4193	.3251	.3640	.5115	.6178	1.1880	.9475	.2282
		6.5	1.1584	.4862	.3651	.4220	.7063	.3041	1.0964	.8510	.0395
		11.0	1.6121	.5413	.4019	.4693	.8510	.0145	1.0176	.7787	-.2200
0	.5	1.0	.8894	.4978	.4317	.4317	.7210	.7981	1.4232	1.1853	.3420
		1.6	1.1463	.5441	.4191	.4731	.9014	.6308	1.3825	1.0741	.2726
		3.0	1.6696	.6160	.4271	.5360	1.2016	.3187	1.3024	.9392	.0774
		6.5	2.7743	.7240	.4681	.6293	1.6592	-.2220	1.1737	.7875	-.4497
		11.0	3.9985	.8129	.5130	.7055	1.9992	-.6972	1.0750	.6929	-1.1219
0	1.0	1.0	1.2326	.5705	0		1.0	.6479	1.4305	.4789	.2923
	.9429	1.6	1.5794	.6184	0		1.2154	.4427	1.3767	.4028	.1737
	.8984	3.0	2.2963	.6964	0		1.5833	.0700	1.2838	.2886	-.1267
	.8719	6.5	3.8245	.8176	0		2.1551	-.5642	1.1456	.1484	-.8942
	.8635	11.0	5.5255	.9187	0		2.5847	-1.1171	1.0438	.0631	-1.8504
-0.5	0.05	1.0	0.1949	0.0888	0.1025	0.1025		1.5623	2.2485	1.8857	0.4620
		1.6	.2760	.1151	.1165	.1263		1.2972	2.0564	1.7066	.4195
		3.0	.4407	.1570	.1419	.1637		.9178	1.8132	1.4796	.3066
		6.5	.7913	.2215	.1846	.2206		.3920	1.5326	1.2242	.0146
		11.0	1.1857	.2752	.2221	.2676		-.0123	1.3551	1.0677	-.3477
-0.5	.5	1.0	.6276	.2247	.2295	.2295		1.0632	1.9917	1.6300	.4397
		1.6	.8723	.2706	.2302	.2698		.7803	1.8493	1.4607	.3255
		3.0	1.3695	.3423	.2482	.3325		.3347	1.6557	1.2454	.0457
		6.5	2.4185	.4503	.2943	.4264		-.3376	1.4198	1.0071	-.6398
		11.0	3.5834	.5387	.3403	.5030		-.8834	1.2658	.8648	-1.4675
-0.5	1.0	1.0	.9692	.2950	0			.7809	1.8781	1.1596	.3441
	.9267	1.6	1.2876	.3409	0			.4968	1.7529	1.0027	.1783
	.8732	3.0	1.9527	.4172	0			.0264	1.5743	.7875	-.2114
	.8451	6.5	3.3846	.5369	0			-.7093	1.3507	.5366	-1.1475
	.8382	11.0	4.9909	.6370	0			-1.3179	1.2037	.3863	-2.7013
-0.75	0.05	1.0	0.1114	0.0274	0.0432	0.0432		2.2475	3.1553	2.6887	0.5841
		1.6	.1759	.0445	.0568	.0621		1.7593	2.7358	2.3090	.5174
		3.0	.3144	.0758	.0802	.0939		1.1702	2.2795	1.8929	.3650
		6.5	.6226	.1294	.1193	.1450		.4753	1.8289	1.4859	.0070
		11.0	.9783	.1769	.1540	.1886		-.0075	1.5736	1.2601	-.4161
-1.0	0.5	1.0	0.4380	0.0673	0.0932	0.0932		1.4401	2.7948	2.2952	0.5728
		1.6	.6534	.0992	.1039	.1262		.9812	2.4731	1.9992	.3938
		3.0	1.1020	.1546	.1259	.1805		.3582	2.1012	1.6434	.0033
		6.5	2.0687	.2456	.1692	.2655		-.4680	1.7143	1.2758	-.8729
		11.0	3.1571	.3242	.2107	.3370		-1.0899	1.4882	1.0688	-1.8783
-1.0	1.0	1.0	.7566	.1168	0			.9450	2.4589	1.8625	.4058
	.9115	1.6	1.0342	.1513	0			.5631	2.2300	1.6073	.1804
	.8488	3.0	1.6290	.2130	0			-.0217	1.9313	1.2746	-.3168
	.8185	6.5	2.9407	.3171	0			-.8679	1.5939	.9052	-1.4450
	.8127	11.0	4.4356	.4078	0			-1.5339	1.3891	.6897	-2.7503

TABLE III

BOUNDARY-LAYER PARAMETERS CALCULATED FOR STAGNATION FLOWS BY USING SUTHERLAND VISCOSITY-TEMPERATURE

RELATION AT PRANDTL NUMBER OF 0.7 WITH NONPOROUS WALL

(a) Body of revolution; $\beta = 0.5$

s	t_w	f_w''	g_w'	θ_w'	ϕ_e	$\left(\dfrac{N_{Nu}}{\sqrt{R_e}}\right)_{\text{3-dimensional}}$	δ_{tr}^*	G_{tr}	θ_{tr}^*	θ_{tr}^*
0.005	0.015	0.2951	0.2518	0.2168	0.1625	0.3066	0.7717	1.0416	0.8924	0.2325
	.050	.3654	.3041	.2623	.2447	.3709	.8582	1.1872	1.0093	.2772
	.070	.3944	.3240	.2797	.2821	.3955	.8839	1.2366	1.0481	.2932
	.100	.4304	.3472	.3000	.3304	.4243	.9081	1.2889	1.0887	.3109
	.150	.4792	.3759	.3253	.3982	.4601	.9288	1.3461	1.1325	.3308
	.200	.5201	.3976	.3446	.4561	.4873	.9371	1.3836	1.1606	.3439
	.250	.5562	.4152	.3602	.5075	.5094	.9388	1.4103	1.1803	.3529
	.300	.5890	.4301	.3734	.5541	.5280	.9366	1.4301	1.1946	.3593
0.02	0.06	0.4115	0.3414	0.2950	0.3202	0.4173	0.9172	1.2882	1.0889	0.3098
	.20	.5292	.4055	.3517	.4823	.4974	.9466	1.4021	1.1746	.3505
	.50	.7041	.4757	.4141	.7210	.5856	.9104	1.4779	1.2281	.3706
0.0625	0.1875	0.5444	0.4223	0.3668	0.5434	0.5187	0.9712	1.4448	1.2068	0.3661
	.625	.7681	.4980	.4341	.8185	.6139	.8877	1.4950	1.2395	.3711
0.2	0.05	0.6134	0.5220	0.4558	0.9317	0.6446	1.1925	1.7611	1.4552	0.4722
	.50	.7240	.4934	.4305	.8250	.6088	.9248	1.5144	1.2546	.3835

(b) Yawed cylinder; $\beta = 1.0$

s	λ	t_w	f_w''	g_w'	θ_w'	$\bar{h}$	ϕ_e	δ_{tr}^*	G_{tr}	θ_{tr}^*	θ_{tr}^*
0.005	1.0	0.015	0.3321	0.2582	0.2218	0.2218	0.1625	0.7352	1.0197	0.8744	0.2291
		.050	.4177	.3125	.2689	.2689	.2447	.8116	1.1603	.9874	.2720
		.100	.5010	.3578	.3084	.3084	.3304	.8508	1.2566	1.0628	.3033
		.200	.6225	.4118	.3558	.3558	.4561	.8628	1.3438	1.1289	.3314
		.300	.7206	.4471	.3870	.3870	.5541	.8482	1.3844	1.1585	.3417
	3.0	.015	.5373	.3164	.2459	.2743	.2787	.5560	.9763	.7934	.1866
		.050	.6912	.3833	.2970	.3327	.4197	.5872	1.1069	.8878	.2103
		.200	1.0963	.5074	.3850	.4412	.7822	.5250	1.2616	.9794	.1993
		.8981	2.2964	.6975	0		1.6262	.0687	1.2860	.2883	-.1281
	11.0	.015	1.1372	.4099	.3058	.3555	.5134	.0985	.8411	.6577	-.1235
		.050	1.4952	.4980	.3695	.4321	.7732	.0272	.9507	.7310	-.2005
		.200	2.5024	.6647	.4780	.5774	1.4411	-.2593	1.0682	.7827	-.5160
		.8622	5.5196	.9211	0		2.9361	-1.1371	1.0494	.0600	-1.8733
0.0625	1.0	0.1875	0.6463	0.4366	0.3782	0.3782	0.5434	0.8959	1.4051	1.1755	0.3528
		.625	.9850	.5228	.4540	.4540	.8185	.7624	1.4358	1.1933	.3350

TABLE IV

BOUNDARY-LAYER PARAMETERS CALCULATED FOR ARBITRARY PRESSURE GRADIENT BY USING LINEAR

VISCOSITY-TEMPERATURE RELATION AT PRANDTL NUMBER OF 1.0 WITH NONPOROUS WALL

(a) Negative pressure gradient; $\beta > 0$

β	t_w	λ	f_w''	θ_w' or g_w'	δ_{tr}^*	G_{tr}	θ_{tr}^*	θ_{tr}^*	β	t_w	λ	f_w''	θ_w' or g_w'	δ_{tr}^*	G_{tr}	θ_{tr}^*	θ_{tr}^*
0.2	0	1.0	0.5233	0.4821	1.1306	1.6479	1.1882	0.4457	1.5	0	1.0	0.6987	0.5147	0.9349	1.5583	1.1215	0.3914
		1.6	.5543	.4891	1.0837	1.6274	1.1730	.4314			1.6	.8233	.5362	.8061	1.5037	1.0811	.3422
		3.0	.6237	.5039	.9852	1.5852	1.1418	.3981			3.0	1.0907	.5772	.5682	1.4088	1.0112	.2249
		6.5	.7839	.5349	.7852	1.5032	1.0813	.3158			6.5	1.6773	.6507	.1634	1.2643	.9052	-.0688
	.5	1.0	.6070	.4951	1.0530	1.6116	1.1611	.4271		.5	1.0	1.1090	.5574	.7200	1.4596	1.0478	.3259
		1.6	.6836	.5082	.9714	1.5757	1.1344	.4014			1.6	1.4348	.5928	.5313	1.3834	.9915	.2330
		3.0	.8506	.5344	.8121	1.5082	1.0844	.3418			3.0	2.1149	.6555	.2120	1.2658	.9051	.0144
		6.5	1.2221	.5845	.5215	1.3935	.9999	.1958			6.5	3.5669	.7592	-.2850	1.1079	.7900	-.5178
	1.0	1.0	.6867	.5069	.9841	1.5801	1.1376	.4082		1.0	1.0	1.4772	.5906	.5579	1.3904	.9963	.2562
		1.6	.8047	.5248	.8762	1.5333	1.1029	.3712			1.6	1.9737	.6350	.3345	1.3050	.9334	.1190
		3.0	1.0578	.5593	.6753	1.4504	1.0416	.2855			3.0	2.9997	.7107	-.0296	1.1800	.8421	-.1984
		6.5	1.6111	.6221	.3300	1.3199	.9456	.0776			6.5	5.1729	.8323	-.5772	1.0213	.7268	-.9547
0.5	0	1.0	0.5811	0.4942	1.0531	1.6130	1.1623	0.4238	2.0	0	1.0	0.7386	0.5206	0.9044	1.5438	1.1106	0.3837
		1.6	.6438	.5070	.9704	1.5773	1.1358	.3961			1.6	.8837	.5444	.7651	1.4849	1.0671	.3287
		3.0	.7811	.5328	.8072	1.5095	1.0857	.3311			3.0	1.1939	.5891	.5114	1.3847	.9932	.1972
		6.5	1.0889	.5828	.5057	1.3930	1.0000	.1703			6.5	1.8712	.6682	.0861	1.2356	.8841	-.1332
	.5	1.0	.7609	.5185	.9168	1.5498	1.1151	.3875		.5	1.0	1.2405	.5686	.6703	1.4364	1.0304	.3101
		1.6	.9167	.5410	.7846	1.4937	1.0735	.3371			1.6	1.6289	.6073	.4699	1.3565	.9714	.2051
		3.0	1.2479	.5833	.5455	1.3983	1.0031	.2195			3.0	2.4366	.6749	.1348	1.2354	.8825	-.0423
		6.5	1.9665	.6577	.1482	1.2557	.8985	-.0671			6.5	4.1561	.7856	-.3816	1.0760	.7666	-.6447
	1.0	1.0	.9277	.5390	.8045	1.4999	1.0780	.3503		1.0	1.0	1.6871	.6052	.4974	1.3632	.9760	.2308
		1.6	1.1648	.5684	.6396	1.4322	1.0279	.2769			1.6	2.2804	.6533	.2624	1.2749	.9111	.0752
		3.0	1.6623	.6215	.3550	1.3237	.9481	.1074			3.0	3.5031	.7345	-.1170	1.1480	.8184	-.2850
		6.5	2.7281	.7111	-.0955	1.1724	.8374	-.2989			6.5	6.0876	.8637	-.6837	.9893	.7033	-1.1424
											6.5	[a]6.0895	[a].8636	[a]-.6835	[a].9893	[a].7033	[a]-1.1417

[a]$\Delta\eta = 0.1$.

TABLE IV.- Concluded

BOUNDARY-LAYER PARAMETERS CALCULATED FOR ARBITRARY PRESSURE GRADIENT BY USING LINEAR

VISCOSITY-TEMPERATURE RELATION AT PRANDTL NUMBER OF 1.0 WITH NONPOROUS WALL

(b) Positive pressure gradient; $\beta < 0$

β	t_w	λ	f''_w	θ'_w or g'_w	δ^*_{tr}	G_{tr}	Θ^*_{tr}	θ^*_{tr}
-0.3264		1.0	0	0.2478	3.4567	2.9751	2.2048	0.6067
-.2800			.2233	.3932	1.8257	1.9707	1.4282	.5912
-.2747		1.6	0	.2580	3.2636	2.8691	2.1119	.6083
-.2000			.3318	.4314	1.5050	1.8172	1.3139	.5380
-.2000	0		.1437	.3616	2.0953	2.1154	1.5370	.6084
-.1943		3.0	0	.2688	3.0713	2.6987	1.9809	.6093
-.1000			.3567	.4394	1.4395	1.7878	1.2921	.5229
-.1094		6.5	0	.2770	2.9338	2.6255	1.9261	.5963
-.1000			.1782	.3789	1.9268	2.0307	1.4737	.5887
-0.2623			0	0.3076	2.5861	2.4071	1.7594	0.6067
-.2500		1.0	.1415	.3778	1.9224	2.0314	1.4747	.5837
-.2000			.2507	.4152	1.6136	1.8747	1.3572	.5472
-.1913			0	.3164	2.4665	2.3463	1.7140	.5923
-.1500		1.6	.2115	.4046	1.6905	1.9151	1.3877	.5541
-.1153	0.5		0	.3235	2.3733	2.2993	1.6789	.5802
-.1000		3.0	.1411	.3834	1.8526	2.0022	1.4534	.5653
-.0500			.3345	.4393	1.4266	1.7854	1.2906	.5133
-.0573		6.5	0	.3279	2.3173	2.2711	1.6579	.5726
-.0500			.1242	.3792	1.8795	2.0191	1.4663	.5634
-0.1988		1.0	0	0.3258	2.3588	2.2870	1.6694	0.5854
-.1366			0	.3316	2.2858	2.2507	1.6423	.5752
-.1000		1.6	.2098	.4086	1.6479	1.8970	1.3744	.5427
-.0500			.3561	.4457	1.3786	1.7630	1.2740	.5030
-.0783	1.0	3.0	0	.3361	2.2308	2.2234	1.6219	.5671
-.0500			.2407	.4179	1.5755	1.8610	1.3475	.5322
-.0377		6.5	0	.3388	2.1979	2.2071	1.6098	.5623
-.0200			.2805	.4283	1.4989	1.8228	1.3188	.5214

TABLE V

CONSTANTS IN INTERPOLATION FORMULAS FOR $\bar{h}$ AND t_{aw}

AS GIVEN BY EQUATIONS (47) AND (48)

ϕ	s	N_{Pr}	λ	$\bar{\alpha}_0$	$\bar{\alpha}_1$	$\bar{\alpha}_2$	$\bar{\beta}_0$	$\bar{\beta}_1$	$\bar{\beta}_2$	$\bar{\gamma}_0$	$\bar{\gamma}_1$	$\bar{\gamma}_2$	$\bar{a}$	$\bar{b}$
1.0	---	1.0	1.0	0.0048	0.04668	-0.01396	-0.05096	-0.12598	0.07776	0.24070	0.72755	0.50667		
			1.6	.01044	.05554	-.02252	-.05734	-.13559	.10708	.21902	.70699	.52485		
			3.0	.01452	.06118	-.03756	-.05850	-.13697	.15428	.18900	.67936	.56027		
			6.5	.01420	.06014	-.06010	-.05106	-.12669	.22183	.15380	.64936	.62539		
1.0	---	.7	1.0	-.02142	.02512	-.01127	.00147	-.08285	.07237	.12590	.51503	.43625	1.0	0
			1.6	-.01479	.04090	-.02156	-.01229	-.10065	.10276	.12118	.50587	.44749	.94443	.03162
			3.0	-.00524	.05727	-.04113	-.02620	-.11404	.15357	.11113	.49072	.47123	.90447	.05008
			6.5	.00119	.06505	-.07135	-.03140	-.11345	.22776	.09456	.47074	.51843	.88384	.05393
---	0.2	.7	1.0	-.04720	.01520	.06139	.05276	-.06336	-.07294	.11252	.50233	.46955	1.0	0
			1.6	-.04480	.02240	.06209	.04264	-.07212	-.05513	.10488	.49636	.49527	.94349	.03163
			3.0	-.03800	.03040	.05428	.03050	-.07672	-.01867	.09435	.48431	.53297	.90124	.04984
			6.5	-.02760	.03440	.03639	.01798	-.07212	.03767	.07961	.46586	.59276	.87874	.05348
			11.0	-.02224	.03648	.01810	.01263	-.06686	.08060	.06974	.45421	.64652	.87303	.05084
---	.02	.7	1.0	.07856	.00692	-.17234	-.19850	-.04647	.39452	.21182	.49208	.27758	1.0	0
			1.6	.08808	.03050	-.20144	-.19490	-.06577	.44192	.19489	.49148	.30249	.94293	.03147
			3.0	.08852	.05326	-.24295	-.17996	-.08105	.51571	.17094	.48562	.33884	.89844	.04964
			6.5	.07904	.06656	-.30069	-.15457	-.08570	.62598	.14149	.47390	.39145	.87192	.05337
			11.0	.06884	.07094	-.35068	-.13502	-.08400	.71785	.12305	.46555	.43428	.86353	.05080

TABLE VI

TYPICAL RESULTS ILLUSTRATING UNIQUENESS PROBLEM FOR POSITIVE PRESSURE GRADIENT

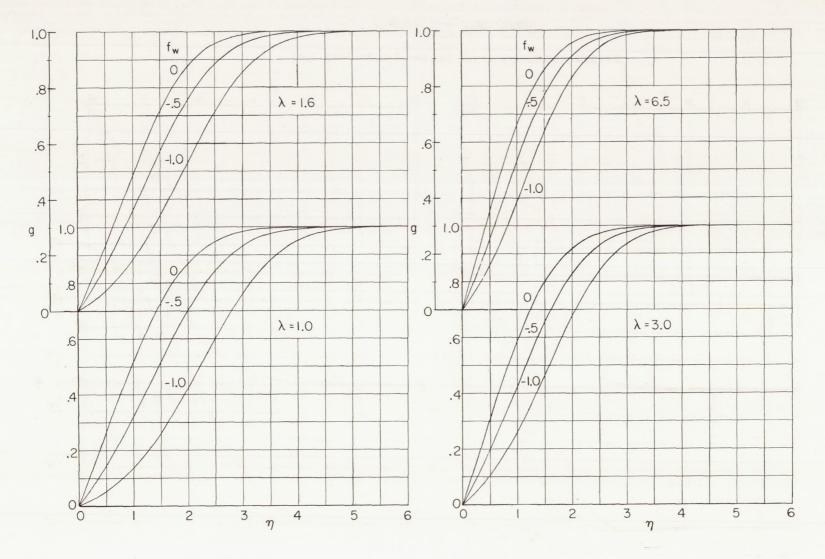$$\left[N_{Pr} = 1.0;\ \lambda = 1.6;\ t_w = 0;\ f_w = 0;\ \beta = -0.2\right]$$

η	f	θ	f'	θ'	f''	$1-f'$	$0.2\,\dfrac{\theta'}{f}$	η	f	θ	f'	θ'	f''	$1-f'$	$0.2\,\dfrac{\theta'}{f}$
0	0	0	0	0.439372	0.345204	1	∞	0	0	0	0	0.431366	0.331800	1	∞
[a]3.8	2.356271	1	1	$.18365 \times 10^{-1}$	$.27782 \times 10^{-1}$	0	0.15588×10^{-2}	4.0	2.497505	0.995654	0.992425	$.12254 \times 10^{-1}$	$.20539 \times 10^{-1}$	0.007575	0.98130×10^{-3}
4.0	2.556748	1.002911	1.004393	$.11241 \times 10^{-1}$	$.16863 \times 10^{-1}$	$-.004393$	$.87932 \times 10^{-3}$	5.0	3.495062	.999835	.999684	$.61629 \times 10^{-3}$	$.11547 \times 10^{-2}$	.000316	$.35266 \times 10^{-4}$
[b]5.0	3.564966	1.006680	1.009436	$.530 \times 10^{-7}$	$-.11370 \times 10^{-3}$	$-.009436$	$.30 \times 10^{-8}$	6.0	4.494981	.999997	.999995	$.11668 \times 10^{-4}$	$.23769 \times 10^{-4}$	.000003	$.5180 \times 10^{-6}$
6.0	4.574128	1.006817	1.008815	$.93471 \times 10^{-5}$	$-.69438 \times 10^{-3}$	$-.008815$	$.4080 \times 10^{-6}$	[a]6.8	5.294980	1	1	$.2490 \times 10^{-6}$	$.5290 \times 10^{-6}$	0	$.94 \times 10^{-8}$
8.0	6.590600	1.006819	1.007754	$.2 \times 10^{-9}$	$-.40457 \times 10^{-3}$	$-.007754$	0	8.0	6.494979	1	1	$.3 \times 10^{-9}$	$-.29 \times 10^{-8}$	0	0
0	0	0	0	.433052	.334808	1	∞	0	0	0	0	.431366	.331800	1	∞
4.0	2.510764	.997029	.995076	$.12016 \times 10^{-1}$	$.19692 \times 10^{-1}$	.004924	$.95716 \times 10^{-3}$	4.0	2.497504	.995654	.992424	$.12254 \times 10^{-1}$	$.20539 \times 10^{-1}$	.007576	$.98130 \times 10^{-3}$
[a]4.4	2.909951	1	1	$.40691 \times 10^{-2}$	$.68033 \times 10^{-2}$	0	$.27960 \times 10^{-3}$	5.0	3.495061	.999836	.999684	$.61629 \times 10^{-3}$	$.11547 \times 10^{-2}$	.000316	$.35266 \times 10^{-4}$
5.0	3.510671	1.001114	1.001825	$.59576 \times 10^{-3}$	$.86387 \times 10^{-3}$	$-.001825$	$.33938 \times 10^{-4}$	6.0	4.494980	.999998	.999995	$.11669 \times 10^{-4}$	$.23782 \times 10^{-4}$	.000005	$.5180 \times 10^{-6}$
[b]5.6	4.111835	1.001258	1.001970	$.61284 \times 10^{-4}$	$-.68378 \times 10^{-4}$	$-.001970$	$.29809 \times 10^{-5}$	[a]7.4	5.894979	1	1	$.97 \times 10^{-8}$	$.244 \times 10^{-7}$	0	$.3 \times 10^{-9}$
6.0	4.512615	1.001270	1.001923	$.11101 \times 10^{-4}$	$-.13916 \times 10^{-3}$	$-.001923$	$.4900 \times 10^{-6}$	8.0	6.494978	1	1	$.3 \times 10^{-9}$	$.35 \times 10^{-8}$	0	0
8.0	6.516206	1.001272	1.001687	$.3 \times 10^{-9}$	$-.91310 \times 10^{-4}$	$-.001687$	0								
								0	0	0	0	.431366	.331800	1	∞
0	0	0	0	.431607	.332251	1	∞	4.0	2.497504	.995654	.992424	$.12254 \times 10^{-1}$	$.20539 \times 10^{-1}$	.007576	$.98130 \times 10^{-3}$
4.0	2.499483	.995833	.992817	$.12218 \times 10^{-1}$	$.20411 \times 10^{-1}$	.007183	$.97764 \times 10^{-3}$	5.0	3.495061	.999836	.999684	$.61629 \times 10^{-3}$	$.11547 \times 10^{-2}$	.000316	$.35266 \times 10^{-4}$
[a]5.0	3.497387	1.0	1	$.61316 \times 10^{-3}$	$.11109 \times 10^{-2}$	0	$.35064 \times 10^{-4}$	6.0	4.494980	.999998	.999995	$.11669 \times 10^{-4}$	$.23783 \times 10^{-4}$	.000005	$.5180 \times 10^{-6}$
[b]6.0	4.497605	1.000161	1.000278	$.11582 \times 10^{-4}$	$-.7174 \times 10^{-6}$	$-.000278$	$.5150 \times 10^{-6}$	[a]8.0	6.494978	1	1	$.3 \times 10^{-9}$	$.39 \times 10^{-8}$	0	0
8.0	6.498131	1.000164	1.000248	$.3 \times 10^{-9}$	$-.13717 \times 10^{-4}$	$-.000248$	0								
								0	0	0	0	.431366	.331800	1	∞
0	0	0	0	.431390	.331846	1	∞	4.0	2.497505	.995654	.992425	$.12254 \times 10^{-1}$	$.20539 \times 10^{-1}$	.007575	$.98130 \times 10^{-3}$
4.0	2.497707	.995670	.992464	$.12250 \times 10^{-1}$	$.20526 \times 10^{-1}$	.007536	$.98090 \times 10^{-3}$	5.0	3.495062	.999835	.999684	$.61629 \times 10^{-3}$	$.11547 \times 10^{-2}$	.000316	$.35266 \times 10^{-4}$
5.0	3.495299	.999850	.999716	$.61597 \times 10^{-3}$	$.11502 \times 10^{-2}$	.000284	$.35244 \times 10^{-4}$	6.0	4.494981	.999997	.999995	$.11668 \times 10^{-4}$	$.23769 \times 10^{-4}$	.000005	$.5180 \times 10^{-6}$
[a]5.6	4.095243	1	1	$.63950 \times 10^{-4}$	$.12343 \times 10^{-3}$	0	$.31231 \times 10^{-5}$	8.0	6.494979	1	1	$.3 \times 10^{-9}$	$-.29 \times 10^{-8}$	0	0
6.0	4.495248	1.000012	1.000024	$.116597 \times 10^{-4}$	$.21262 \times 10^{-4}$	$-.000024$	$.5180 \times 10^{-6}$	[a]8.6	7.094979	1	1	0	$-.32 \times 10^{-8}$	0	0
[b]6.6	5.095264	1.000015	1.000027	$.6871 \times 10^{-6}$	$-.5795 \times 10^{-6}$	$-.000027$	$.270 \times 10^{-7}$	10.4	8.894978	1	1	0	$-.25 \times 10^{-8}$	0	0
8.0	6.495300	1.000015	1.000025	$.3 \times 10^{-9}$	$-.14143 \times 10^{-5}$	$-.000025$	0								
								0	0	0	0	.431366	.331800	1	∞
0	0	0	0	.431376	.331820	1	∞	4.0	2.497505	.995654	.992424	$.12254 \times 10^{-1}$	$.20539 \times 10^{-1}$	.007576	$.98130 \times 10^{-3}$
4.0	2.497592	.995660	.992442	$.12252 \times 10^{-1}$	$.20533 \times 10^{-1}$	.007558	$.98110 \times 10^{-3}$	5.0	3.495061	.999836	.999684	$.61629 \times 10^{-3}$	$.11547 \times 10^{-2}$	.000316	$.35266 \times 10^{-4}$
5.0	3.495164	.999842	.999698	$.61615 \times 10^{-3}$	$.11528 \times 10^{-2}$	.000302	$.35256 \times 10^{-4}$	6.0	4.494981	.999997	.999995	$.11669 \times 10^{-4}$	$.23775 \times 10^{-4}$	.000005	$.5180 \times 10^{-6}$
[a]5.8	4.295096	1	1	$.27841 \times 10^{-4}$	$.54710 \times 10^{-4}$	0	$.12964 \times 10^{-5}$	8.0	6.494979	1	1	$.3 \times 10^{-9}$	$-.8 \times 10^{-9}$	0	0
6.0	4.495096	1.000004	1.000007	$.116651 \times 10^{-4}$	$.22684 \times 10^{-4}$	$-.000007$	$.5180 \times 10^{-6}$	[a]9.2	7.694978	1	1	0	$-.12 \times 10^{-8}$	0	0
[b]6.8	5.295104	1.000006	1.000012	$.2491 \times 10^{-6}$	$-.2982 \times 10^{-6}$	$-.000012$	$.94 \times 10^{-8}$	10.4	8.894978	1	1	0	$-.10 \times 10^{-8}$	0	0
8.0	6.495117	1.000006	1.000011	$.3 \times 10^{-9}$	$-.6145 \times 10^{-6}$	$-.000011$	0								
								0	0	0	0	.431366	.331800	1	∞
0	0	0	0	.431370	.331808	1	∞	4.0	2.497505	.995654	.992424	$.12254 \times 10^{-1}$	$.20539 \times 10^{-1}$	.007576	$.98130 \times 10^{-3}$
4.0	2.497540	.995656	.992432	$.12253 \times 10^{-1}$	$.20537 \times 10^{-1}$	.007568	$.98120 \times 10^{-3}$	5.0	3.495061	.999836	.999684	$.61629 \times 10^{-3}$	$.11547 \times 10^{-2}$	.000316	$.35266 \times 10^{-4}$
5.0	3.495103	.999838	.999690	$.61623 \times 10^{-3}$	$.11539 \times 10^{-2}$	.000310	$.35262 \times 10^{-4}$	6.0	4.494981	.999998	.999995	$.11669 \times 10^{-4}$	$.23775 \times 10^{-4}$	.000005	$.5180 \times 10^{-6}$
[a]6.0	4.495028	1	1	$.11667 \times 10^{-4}$	$.23327 \times 10^{-4}$	0	$.5191 \times 10^{-6}$	8.0	6.494979	1	1	$.3 \times 10^{-9}$	$-.22 \times 10^{-8}$	0	0
[b]7.0	5.495032	1.000002	1.000005	$.873 \times 10^{-7}$	$-.1354 \times 10^{-6}$	$-.000005$	$.32 \times 10^{-8}$	[a]9.8	8.294978	1	1	0	$-.22 \times 10^{-8}$	0	0
8.0	6.495036	1.000002	1.000005	$.3 \times 10^{-9}$	$-.2584 \times 10^{-6}$	$-.000005$	0	10.4	8.894978	1	1	0	$-.20 \times 10^{-8}$	0	0
0	0	0	0	.431368	.331803	1	∞	0	0	0	0	.431366	.331800	1	∞
4.0	2.497519	.995655	.992427	$.12253 \times 10^{-1}$	$.20538 \times 10^{-1}$	.007573	$.98121 \times 10^{-3}$	4.0	2.497504	.995654	.992424	$.12254 \times 10^{-1}$	$.20539 \times 10^{-1}$	.007576	$.98130 \times 10^{-3}$
5.0	3.495078	.999836	.999687	$.61627 \times 10^{-3}$	$.11544 \times 10^{-2}$	.000313	$.35264 \times 10^{-4}$	5.0	3.495061	.999836	.999684	$.61629 \times 10^{-3}$	$.11547 \times 10^{-2}$	.000316	$.35266 \times 10^{-4}$
6.0	4.494999	.999998	.999997	$.11668 \times 10^{-4}$	$.23597 \times 10^{-4}$	.000003	$.5180 \times 10^{-6}$	6.0	4.494980	.999998	.999995	$.11669 \times 10^{-4}$	$.23780 \times 10^{-4}$	.000005	$.5180 \times 10^{-6}$
[a]6.2	4.694999	1	1	$.47090 \times 10^{-5}$	$.95670 \times 10^{-5}$	0	$.2006 \times 10^{-6}$	8.0	6.494978	1	1	$.3 \times 10^{-9}$	$.20 \times 10^{-8}$	0	0
[b]7.2	5.695000	1	1	$.296 \times 10^{-7}$	$-.564 \times 10^{-7}$	0	$.52 \times 10^{-8}$	[a]10.4	8.894978	1	1	0	$.10 \times 10^{-8}$	0	0
8.0	6.495001	1	1	$.3 \times 10^{-9}$	$-.1029 \times 10^{-6}$	0	0								

[a]Denotes value of η at which convergence procedure of reference 21 was applied.

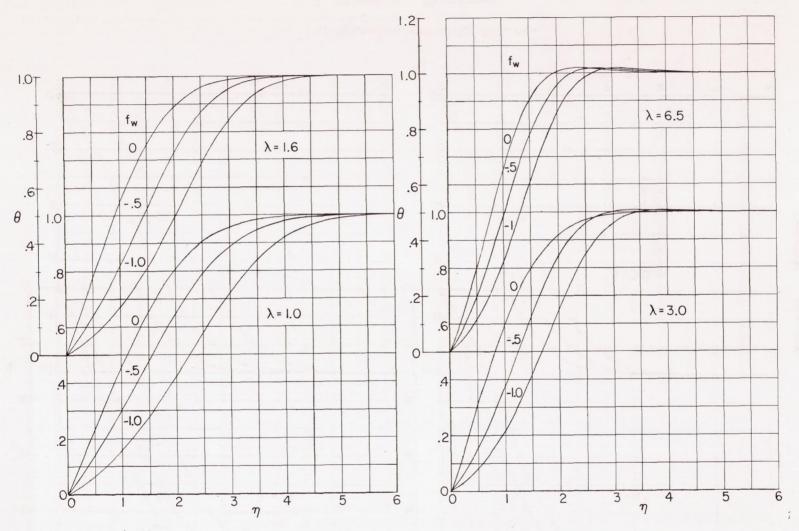[b]Denotes value of η at which f'' first became negative.

(a) Chordwise velocity ratios.

Figure 1.- Typical nondimensional velocity and stagnation-enthalpy-difference profiles. $\phi = 1.0$; $\beta = 1.0$; $N_{Pr} = 0.7$; $t_w = 0.5$.

(b) Spanwise velocity ratios.

Figure 1.- Continued.

(c) Stagnation-enthalpy-difference ratios.

Figure 1.- Concluded.

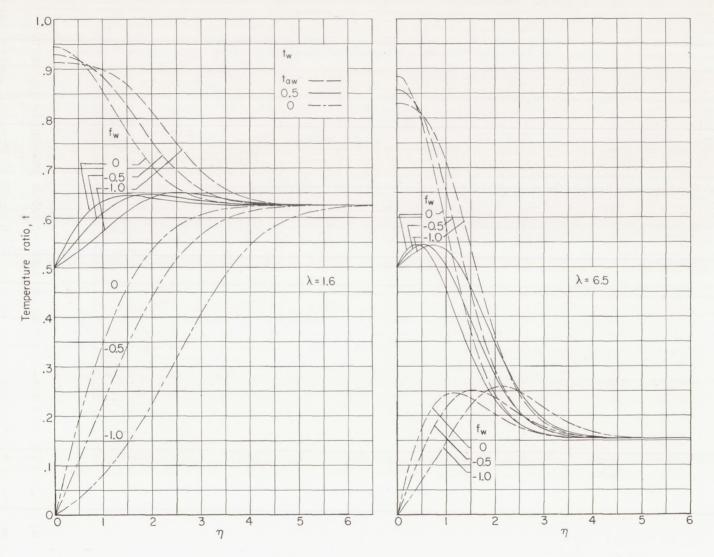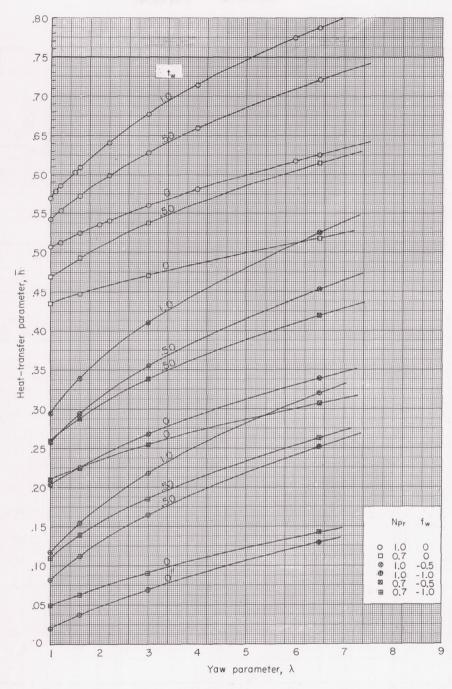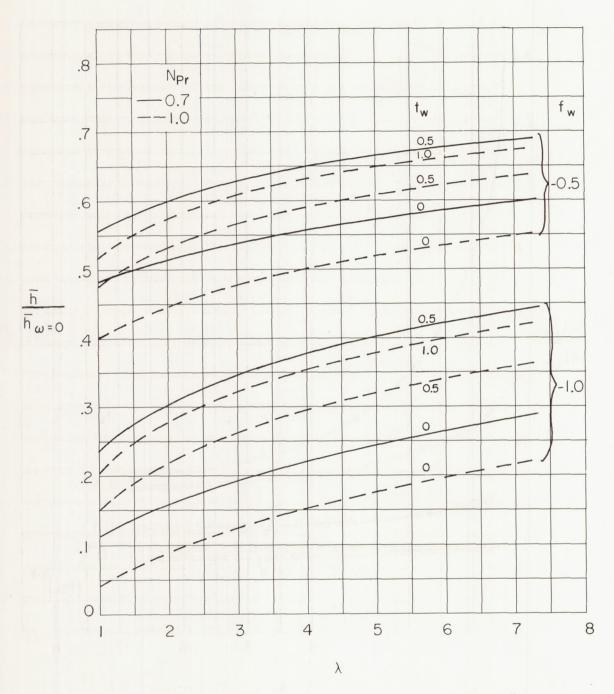Figure 2.- Ratios of local static temperature to total stagnation temperature. $\phi = 1.0$; $\beta = 1.0$; $N_{Pr} = 0.7$.
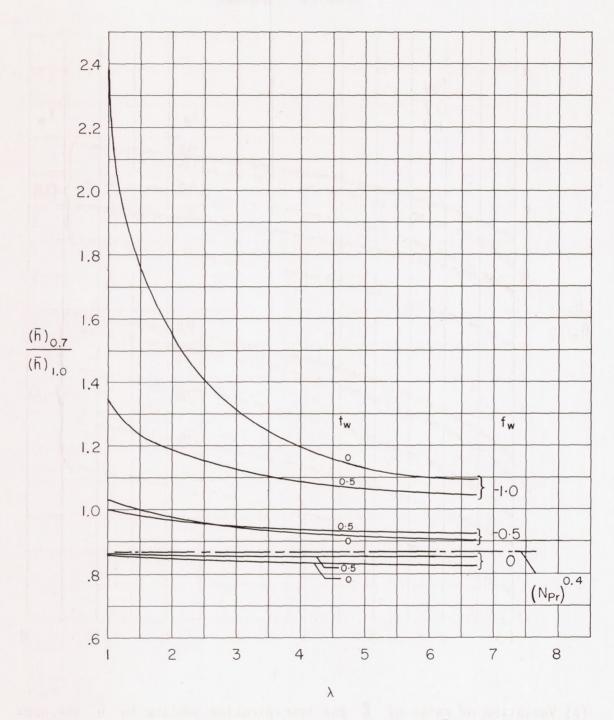
(a) Variation of heat-transfer parameter with yaw-angle parameter.

Figure 3.- Effect of yaw angle, stream Mach number, Prandtl number, and
   transpiration cooling on heat-transfer coefficient at stagnation line.
   $\phi = 1.0$; $\beta = 1.0$.

(b) Variation of ratio of $\bar{h}$ for transpiration cooling to $\bar{h}$ for non-porous wall with yaw-angle parameter.

Figure 3.- Continued.

(c) Variation of ratio of $\bar{h}$ for $N_{Pr} = 0.7$ to $\bar{h}$ for $N_{Pr} = 1.0$ with yaw-angle parameter.

Figure 3.- Concluded.
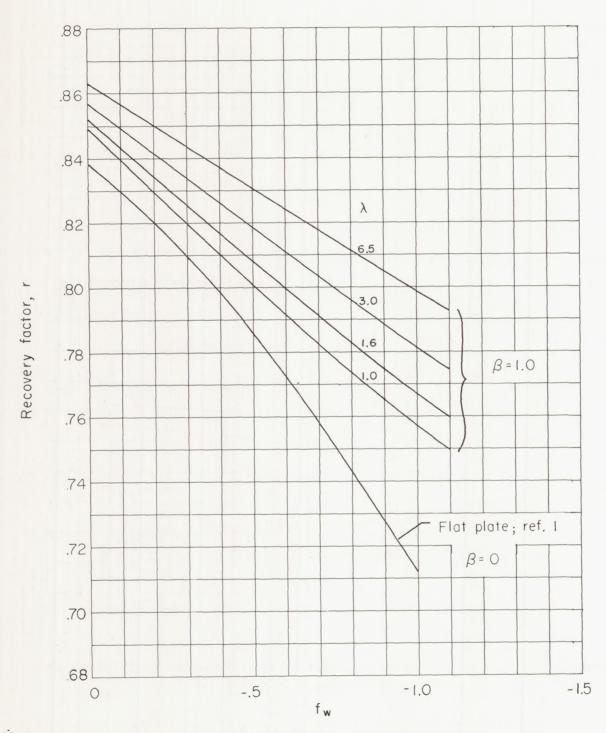
Figure 4.- Effect of transpiration cooling on recovery factor. $\phi = 1.0$.
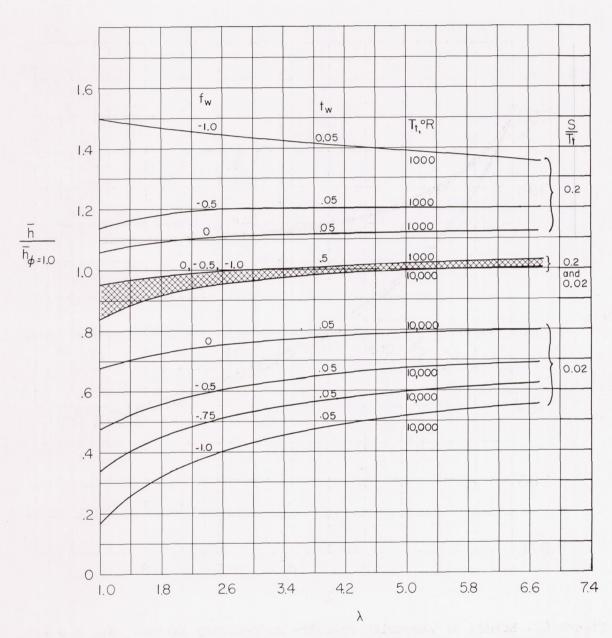
Figure 5.- Effect of viscosity relation on heat-transfer coefficient at stagnation line. $N_{Pr} = 0.7$; $\beta = 1.0$.
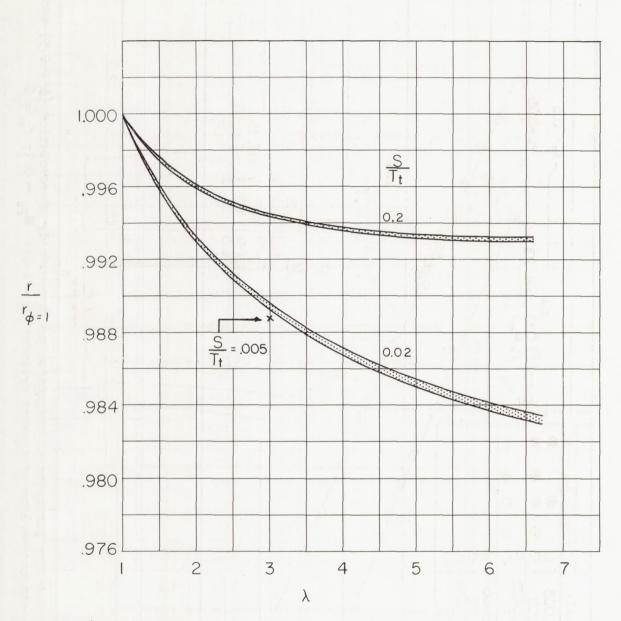
Figure 6.- Effect of viscosity relation on recovery factor. $N_{Pr} = 0.7$;
$\beta = 1.0$.
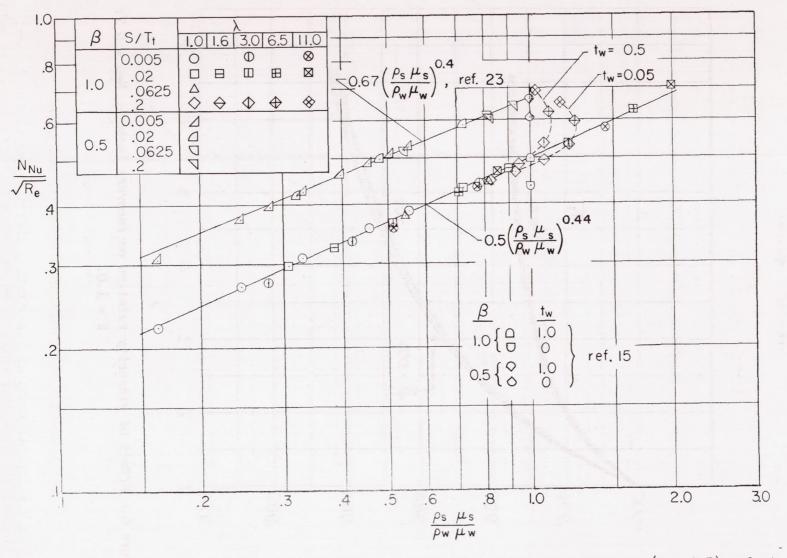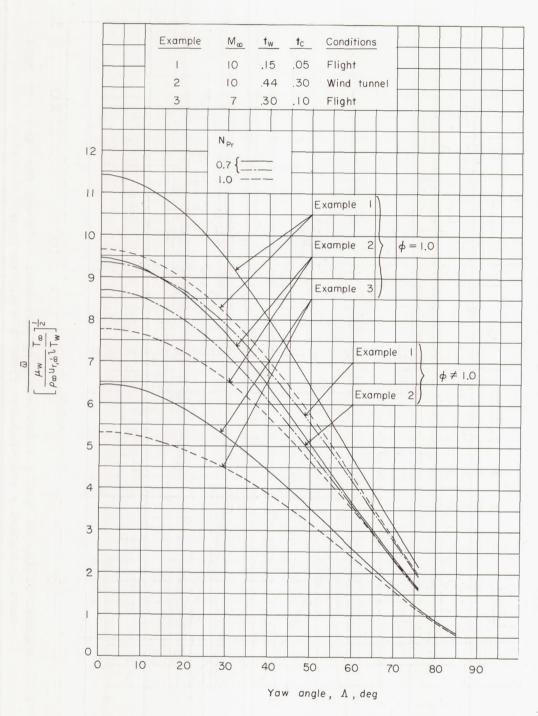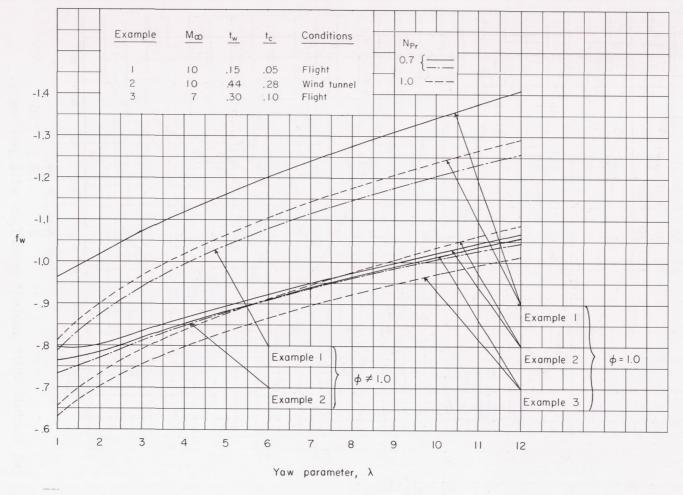
Figure 7.- Heat-transfer parameter at stagnation point on a body of revolution (β = 0.5) and at the stagnation line of a yawed cylinder (β = 1.0). $N_{Pr} \approx 0.7$; $f_w = 0$.

(a) Variation of coolant mass flow with yaw angle.

Figure 8.- Typical examples illustrating effect of yaw angle, Prandtl number, and viscosity relation on coolant mass flow required to maintain a constant wall temperature.

(b) Effect of compressibility on transpiration-cooling parameter. Curves for $\phi = 1.0$ have been arbitrarily extrapolated from $\lambda = 6.5$ to 11.0.
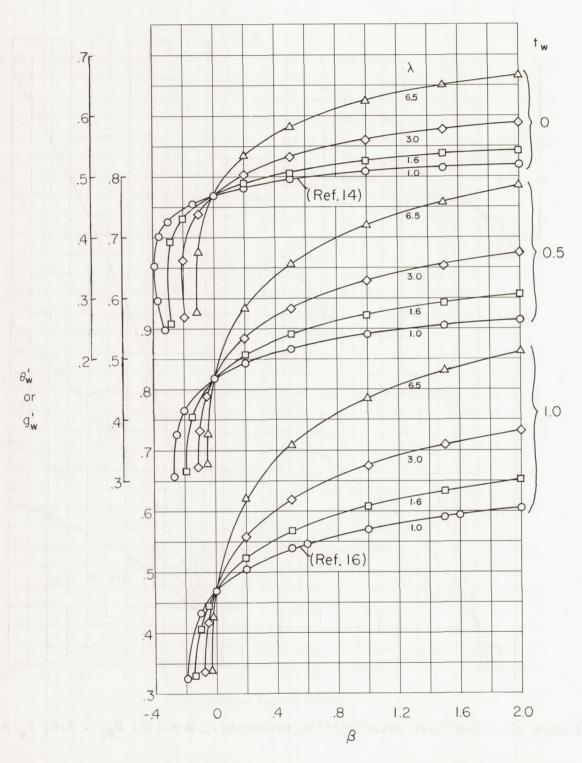
Figure 8.- Concluded.

Figure 9.- Variation of heat-transfer and spanwise skin-friction parameters with pressure-gradient parameter. $\phi = 1.0$; $N_{Pr} = 1.0$; $f_w = 0$.
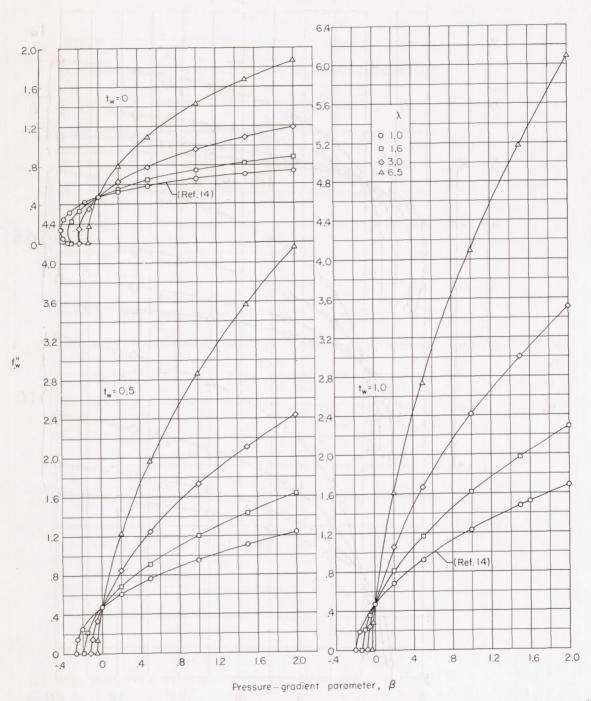
Figure 10.- Chordwise skin-friction parameter. $\phi = 1.0$; $N_{Pr} = 1.0$; $f_w = 0$.
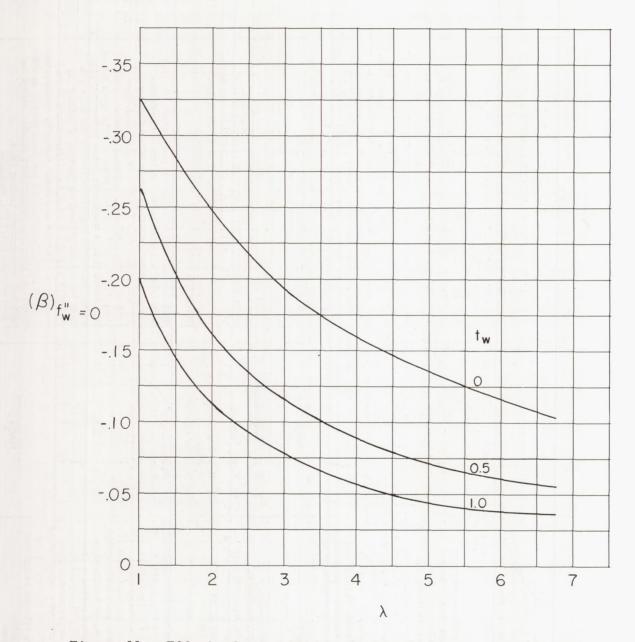
Figure 11.- Effect of yaw and wall temperature on pressure gradient required for chordwise separation. $\phi = 1.0$; $N_{Pr} = 1.0$; $f_w = 0$.